RESEARCH MEMORANDUM

LONGITUDINAL STABILITY CHARACTERISTICS IN MANEUVERING FLIGHT OF THE CONVAIR XF-92A DELTA-WING AIRPLANE INCLUDING THE EFFECTS OF WING FENCES

By Thomas R. Sisk and Duane O. Muhleman

High-Speed Flight Station
Edwards, Calif.

NATIONAL ADVISORY COMMITTEE
FOR AERONAUTICS

WASHINGTON

January 13, 1955

NATIONAL ADVISORY COMMITTEE FOR AERONAUTICS

RESEARCH MEMORANDUM

LONGITUDINAL STABILITY CHARACTERISTICS IN MANEUVERING FLIGHT OF THE CONVAIR XF-92A DELTA-WING AIRPLANE INCLUDING THE EFFECTS OF WING FENCES

By Thomas R. Sisk and Duane O. Muhleman

SUMMARY

The longitudinal stability characteristics of the Convair XF-92A delta-wing airplane in maneuvering flight were investigated as a part of a flight research program conducted by the National Advisory Committee for Aeronautics. This investigation included the determination of the characteristics of the basic airplane and also the effects of two wing fence configurations on these characteristics. One fence extended over the upper surface from the hinge line to the leading edge, and the other extended from the hinge line around the leading edge to the lower surface. The tests covered the Mach number range from 0.70 to 0.95 at altitudes from 22,000 to 39,000 feet.

Over the Mach number range tested, the airplane experienced a marked decrease in stability at moderate lift in the form of a pitch-up which appeared to be oscillatory in nature. The region of reduced stability covered a relatively small angle-of-attack range, and steady flight above and below this region was possible. The lower boundary of this region decreased in normal-force coefficient from 0.40 to 0.15 as the Mach number increased from 0.70 to 0.95.

The longitudinal oscillations encountered in the region of reduced stability attained an amplitude of ± 1 g. In addition, excessive negative load factors were encountered during the recovery from some of the turns as a result of the low damping, high control effectiveness, and poor characteristics of the hydraulic control system.

The speed loss during some of the maneuvers could cause an incremental change in load factor in excess of 1 g as a result of out-of-trim conditions. This speed instability was felt by the pilots to be easily controllable.

There was no apparent pitch-up in the usable lift range at Mach numbers below 0.70 with the wing fences installed. The improvement derived from the fences decreased with an increase in Mach number until no difference in the stability characteristics could be noted between the fence configurations and the basic airplane at Mach numbers above approximately 0.90. No appreciable difference in stability characteristics was noted between the two fence configurations tested.

INTRODUCTION

The Convair XF-92A airplane was originally constructed to determine the handling characteristics, primarily at low speed, of an airplane having a delta-wing configuration. In view of the interest in delta-wing airplanes for high-speed flight, a more powerful power plant was installed in the XF-92A and the flight envelope was extended to sonic speed during the subsequent cooperative program by the NACA and the Air Force. Upon completion of these tests the XF-92A was assigned to the NACA for general research.

Preliminary flight results covering the longitudinal stability and control and the dynamic longitudinal stability characteristics at approximately level-flight lift coefficients have been reported in references 1 and 2, respectively. The results of these investigations showed no adverse stability or trim characteristics other than low longitudinal damping. The present paper is concerned primarily with the longitudinal stability of the airplane in turning flight. Results are presented for the airplane without wing fences and also with wing fences located at 60 percent of the wing semispan and these results are compared with the basic airplane configuration. The tests were made in the period from April to August, 1953 at the NACA High-Speed Flight Station at Edwards Air Force Base, Calif.

SYMBOLS

C_m	pitching-moment coefficient due to static stability
C_m'	total aerodynamic pitching-moment coefficient
$C_{m_{\dot{\alpha}}}$	damping derivative, $\frac{dC_m}{d\frac{\dot{\alpha}\bar{c}}{2V}}$
$C_{m_{\delta_e}}$	control effectiveness parameter, $dC_m/d\delta_e$

[redacted]

$C_{m_{\dot{\theta}}}$	damping derivative, $\frac{dC_m}{d\frac{\dot{\theta}\bar{c}}{2V}}$
C_{N_A}	airplane normal-force coefficient, Wn/qS
c	wing chord, ft
$\bar{c}$	wing mean aerodynamic chord (M.A.C.), ft
F_e	longitudinal stick force, lb
g	acceleration due to gravity, ft/sec^2
h_p	pressure altitude, ft
I_Y	airplane moment of inertia in pitch, slug-ft^2
M	Mach number
n	normal acceleration, g units
q	dynamic pressure, lb/sq ft
S	wing area, sq ft
t	time, sec
t_{max}	maximum wing thickness at any span station, in.
V	forward velocity, ft/sec
W	airplane weight, lb
α	angle of attack, deg
$\dot{\alpha}$	$d\alpha/dt$
δ_e	longitudinal control angle, $\frac{\delta_{e_L} + \delta_{e_R}}{2}$, deg
δ_s	longitudinal stick position, in.
$\dot{\theta}$	pitching angular velocity, radians/sec

[redacted]

$\ddot{\theta}$ pitching angular acceleration, radians/sec^2

Subscripts:

L left

R right

1 initial conditions

AIRPLANE

The Convair XF-92A is a semitailless delta-wing airplane having 60° leading-edge sweepback of the wing and vertical stabilizer. The elevons and rudder are full-span constant-chord surfaces and are 100 percent hydraulically boosted. The artificial "feel" system provides forces approximately proportional to deflection and is adjustable in flight by the pilot. Trim is accomplished by changing the control stick position at which zero stick force is obtained. The airplane has no leading- or trailing-edge slats or flaps, no dive brakes, and no trim tabs. Table I lists the physical characteristics and figure 1 shows a three-view drawing of the airplane. Photographs are presented in figure 2.

Two wing fence configurations located at 60.7 percent of the wing semispan were installed on the airplane for part of the tests presented in this paper. Both fence configurations are illustrated in figure 3. The first configuration (basic fence) extended over the upper surface from the elevon hinge line to the leading edge. Its height was constant between wing-chord stations 10.15 and 50.90 and equal to the maximum wing thickness at the fence span station. The second fence configuration (modified fence) extended the original configuration around the leading edge to wing-chord station 1.95 from which point it was faired into the lower surface at wing-chord station 20.30.

The hydraulic control system of the XF-92A is characterized by high friction and break-out forces and appreciable lag and overshoot of elevon-to-stick motion. Figure 4(a) illustrates the stick-force gradient and friction forces for three feel settings from ground calibrations with no load on the elevon (a feel setting of 5 was the setting generally used for the maneuvers presented). The rates used for the calibration were approximately 5° per second. Figure 4(b) illustrates the positioning error of elevon-to-stick motion and figure 4(c) shows the results of these characteristics on a typical flight maneuver. It should be noted at the beginning of the maneuver that the elevon angle increases 0.4° as the force decreases from approximately 6.5 to 2.5 pounds. Also, near the end of the maneuver the elevon angle increases approximately 1.5° with constant

(17.5 pounds) control force. Control system characteristics such as shown in figure 4 preclude the execution of precise maneuvers and make difficult the analysis of the subsequent data.

INSTRUMENTATION AND ACCURACY

The XF-92A airplane is equipped with standard NACA recording instruments for recording airspeed, altitude, normal acceleration, pitching angular velocity, control positions, stick and pedal positions and forces, sideslip angle, and angle of attack. All instruments are correlated by a common timer.

The airspeed installation was calibrated using the radar phototheodolite method of reference 3. The low-speed static pressure calibration needed for the pressure survey in the method was obtained from an Air Force F-86 pacer airplane and the pressure surveys were checked with radiosonde balloon data. This calibration method resulted in a Mach number accuracy of ±0.01.

Corrections were applied to the angle-of-attack measurements to account for the error caused by the inertia loads on the nose boom on which the angle-of-attack vane is located. This error amounted to 0.16° per g and was determined by statically loading the boom to simulate inertia loads up to 7g. No corrections were made for vane floating, pitching velocity, or upwash. The maximum error in angle of attack resulting from pitching velocity is of the order of 0.8°. The estimated accuracy of the angle-of-attack recorder is ±0.5°.

Reading accuracies of the other pertinent recorded quantities are:

$\dot{\theta}$, radians per sec	±0.02
$\ddot{\theta}$, radians per sec^2	±0.05
n, g units	±0.05
δ_e, deg	±0.20
δ_s, in.	±0.20
F_e, lb	±1.00

The weight was obtained from the pilot's reading of fuel quantity gages at each maneuver and is believed accurate to ±100 pounds.

TESTS, RESULTS, AND DISCUSSION

The longitudinal stability characteristics in maneuvering flight were measured in wind-up turns, that is, turns in which acceleration is gradually increased at constant speed, over the Mach number range from 0.70 to 0.95 at altitudes from 22,000 to 39,000 feet with most of the data being obtained between 30,000 and 35,000 feet. The wind-up turn maneuver was utilized in place of straight pull-ups in an attempt to perform constant-speed maneuvers. In some cases as much as 3,000 feet in altitude was lost during a specific maneuver in attempting to hold the speed constant. The considerable differences in altitude between runs resulted from the short operational time available at altitude. The altitudes listed on the subsequent figures are the initial altitudes for the maneuvers shown. The center of gravity for these tests varied between 27.2 and 28.7 percent of the mean aerodynamic chord.

Basic Airplane

Stability characteristics at constant Mach number.- The first wind-up turns performed with the XF-92A indicated a pitch-up as shown at about time 11 seconds of the time history in figure 5. Examination of the maneuver indicates that the airplane started to recover between time 11.5 and 12 seconds and then more control was applied to increase acceleration again. The behavior at the pitch-up indicates that the pitch-up might be of an oscillatory nature. In order to investigate the characteristics of the airplane in the stability-change region, constant-acceleration turns were performed at lift coefficients below and slightly above the stability break at Mach numbers of about 0.70 and 0.85. These turns are presented in figure 6. The first part of figure 6(a), (time 0 to 9, sec) and figure 6(b) show the airplane to be quite steady at acceleration levels below the stability break at both Mach numbers. The latter part of figure 6(a) and figure 6(c) show the airplane to be oscillatory at the higher acceleration levels at both Mach numbers with the more pronounced oscillation at $M \approx 0.70$. There is some damping indicated in both oscillations. It appears then, from an inspection of figures 5 and 6, that the airplane handles satisfactorily at the lower lift coefficients. At moderate to relatively low values of lift coefficient a decrease in stability occurs. The angle-of-attack range for which the decreased stability is present is apparently relatively small.

To establish the variation with Mach number of the lift coefficient for the stability decrease, wind-up turns were made at Mach numbers between 0.70 and 0.95. Representative turns at Mach numbers of 0.70, 0.80, 0.85, 0.90, and 0.95 are shown in figure 7. Failure of the instrument for obtaining the pitching angular acceleration of the turn of figure 7(a) prevented the calculation of pitching-moment coefficients

and figure 5 is therefore utilized for the calculations at $M \approx 0.70$. It is evident from an inspection of the time histories that the maneuvers are not as smoothly executed as might be desired. The disturbances result both from the change in stability encountered at moderate lift and the poor characteristics of the control system discussed previously.

The variation of longitudinal control angle and stick force with angle of attack and normal acceleration along with the static pitching-moment-coefficient variation with angle of attack and C_{N_A} are presented in figure 8. The pitching-moment-coefficient variations shown in figure 8 were calculated from the data obtained during each run by the method outlined in the Appendix. The variation of longitudinal control angle with angle of attack presented in figure 8 and the time histories of figure 7 indicate that all the turns are generally characterized by a region of reasonably linear variation of δ_e with α at low lift followed by a region of reduced stability at moderate lift in which a pitch-up occurs. The degree of severity of the pitch-up appeared to be a function of the rate of control input - the more extreme pitch-ups occurring at the higher rates. The degree of severity of the pitch-up was also undoubtedly aggravated by the poor control system and the low damping of the airplane. In analyzing the data, the lift coefficient at which the stability started to deteriorate from its low-lift linear value was selected as the point to define a stability boundary, and is indicated by ticks on the plots of δ_e against α of figure 8. Beyond this break the α variation with δ_e is no longer a measure of stability because it is affected by pitching acceleration (and unknown control effectiveness). In correlating this boundary with the pilot's opinions, it was found that the pilot reported the behavior unacceptable at a slightly higher load factor than that defined by the boundary in every case. Since the points selected are clearly defined and correlate reasonably well with the pilot's opinions, they are used to define the stability boundary. The ticks on the curves defining the variation of C_m with α and C_{N_A} show the point of stability decrease as determined from the curve of δ_e against α. The pitching-moment curves are dashed above $\alpha \approx 12^\circ$ because of the uncertainty of the variation of the control-effectiveness parameter with lift. It may be noted that no marked region of instability is apparent in the calculated pitching-moment-coefficient variations even though the variations of δ_e with α and time histories point out the severity of the conditions that exist; however, the pitching-moment-coefficient variation does show a reduction in stability at about the same angle of attack as the variations of δ_e with α. It may be noted here that unpublished wing-loads data on the XF-92A indicate the same abrupt stability change over the same small angle-of-attack range as shown by the curves of figure 8. It is evident, then, that for a delta-wing configuration, even minor variations in the pitching-moment shape

[redacted]

might be objectionable. The stick-force variation is presented in figure 8 to point out the irregularity associated with the artificial feel system installed in the airplane and to reiterate the high friction and break-out forces encountered. It should be noted that the force gradient should not be taken as the true variation with Mach number since all maneuvers were not executed with the same feel setting.

Figure 9 presents the stability boundary that defines the region of unsatisfactory maneuvering stability as the variation of airplane normal-force coefficient with Mach number. This boundary was determined from all flight data including the representative data of figure 7. The boundary decreases from a normal-force coefficient of approximately 0.40 at $M = 0.70$ to a normal-force coefficient of approximately 0.15 at $M = 0.95$. The boundary showing the maximum airplane normal-force coefficient obtained during the tests (inadvertently as well as intentionally) is also presented in figure 9. The stability boundaries of the X-5 airplane having 59° sweepback and a fighter airplane having 35° sweepback as obtained from references 4 and 5, respectively, are also shown in figure 9 for comparison with the XF-92A. The boundary for the XF-92A occurs at appreciably lower lift (and also lower angle of attack) than for the other airplanes. The pitch-up occurs at a comparable load factor, however, because of the lower wing loading of the XF-92A. To the pilot, the deterioration of stability and controllability is virtually intolerable and often was more disconcerting than the pitch-up encountered on the X-5 and the 35° swept-wing airplanes.

As stated at the outset of this section, the airplane behavior at the boundary appeared oscillatory in nature and in some cases these oscillations became quite large in amplitude. Figure 10 is a time history of an oscillation during which the pilot attempted to hold the controls fixed. (Fig. 10 is actually a continuation of the time history of fig. 7(d).) Actually there was considerable motion of the stick which affected the airplane somewhat. From figure 10, the pitching oscillation is seen to have a period of approximately 2 seconds and an almost constant amplitude of approximately ± 1 g. There is a considerable variation in the longitudinal control angle which possibly affected the response somewhat, although the pilot was attempting to hold the controls fixed. Although this does not appear to be dangerous for the XF-92A, it does preclude the execution of precise maneuvers such as gunnery tracking in this lift region. Under some conditions of speed, altitude, or wing loading it would be possible for this oscillation coupled with the pitch-up to cause the limit load factor of the airplane to be exceeded.

Another potentially dangerous characteristic evidenced during the course of the investigation was associated with the application of corrective control following a pitch-up. The low damping of the tailless configuration and the high control effectiveness coupled with the poor characteristics of the control system made it possible to develop excessively

high negative load factors during the recovery. Figure 11 presents a wind-up turn in which a negative load factor of 4.5g was reached during the recovery from an inadvertent pitch-up to nearly 8g.

The data shown indicate that at moderate lift there exists a small angle-of-attack range of markedly reduced stability and that the airplane behavior in this range is partly a function of rates of entry. These data suggest that steady flight above the boundary might be possible. Figure 12 presents a time history of a wind-up turn in this region. The stability boundary was penetrated at $M \approx 0.95$ and steady flight was maintained as the speed decreased until an abrupt trim change was encountered at $M \approx 0.86$. The stability boundary is noted on the figure for convenience.

Stability characteristics with varying Mach number.- The previous discussion has dealt with the maneuvering stability as affected by lift coefficient and angle of attack. All the maneuvers that were presented, however, had some speed loss that could not be prevented. The following data are presented, therefore, to evaluate the speed stability in the region of the trim change and to give a measure of its effect when superimposed on the lift and angle-of-attack stability. The variation of longitudinal control angle with Mach number for 1 g, 2g, and 3g corrected to an altitude of 35,000 feet is presented in figure 13. An inspection of figure 13 shows that it is possible to reach an out-of-trim condition, with controls fixed, that would subject the airplane to an incremental load factor in excess of 1 g during speed losses at Mach numbers between 0.83 and 0.90 depending on the normal acceleration factor. The wind-up turn of figure 12 substantiates qualitatively the data of figure 13. Figure 12 shows that the load factor increases about $1\frac{1}{2}$ g as the speed decreases from $M \approx 0.86$ to $M \approx 0.83$ with the controls fixed. It was the pilot's opinion, however, that the speed instability is of considerably less importance than the pitch-up at constant speed because the speed instability develops slowly and is easily controlled.

Fence Configurations

Wind-tunnel tests of a model of similar plan form but having a thinner airfoil section indicated that a fence configuration showed promise in improving the maneuvering stability characteristics. Two wing fence configurations located at 60.7 percent of the wing semispan were installed on the XF-92A and tested. The location of the fences was selected on the basis of the wind-tunnel tests. The physical dimensions of the fences are defined under the section "AIRPLANE" and a sketch of the fences is presented in figure 3.

Sufficient Mach number coverage was not obtained to compare the two fence configurations at all Mach numbers presented for the basic airplane since the program was terminated abruptly when the airplane was damaged in a taxiing accident. There was enough duplication of maneuvers, however, to show that no appreciable differences existed in the stability characteristics between the two fence configurations. The two configurations are therefore presented together and an analysis parallel to that made for the basic airplane is presented.

Figure 14 presents representative time histories of wind-up turns with wing fences installed. Both fence configurations were evaluated at Mach numbers of 0.70, 0.85, and 0.90 and, therefore, both sets of data are presented for comparison. These time histories bear out the pilot's comments that at the lower Mach numbers the fence-configuration maneuvers were considerably steadier than were the maneuvers of the basic airplane. It may be noted in figures 14(a) and (b) at $M \approx 0.70$ that the maneuvers were continued to full up longitudinal control angle which corresponded to angles of attack in excess of 30° before recovery was initiated. However, as indicated, these maneuvers involved considerable speed loss at angles of attack above about 20°.

The data presented in figure 15 include the basic airplane static pitching-moment-coefficient variation with angle of attack for comparison with the fence results. The analysis plots are terminated at an angle of attack of 20° because of the large speed loss at the higher angles and the curves are dashed in the higher angle-of-attack range to denote the uncertainty of the $C_{m_{\delta_e}}$ values as previously mentioned. Analysis of these figures shows that there is no apparent pitch-up in the usable lift range at Mach numbers below about $M = 0.80$. The improvement derived from the fence configuration decreases with an increase in Mach number, however, until no difference in the stability characteristics could be noted between the fence configurations and the basic airplane above $M \approx 0.90$.

Figure 16 presents the stability boundary for the wing-fence installation and compares this boundary to that obtained for the basic airplane. This boundary, as in the case of the basic airplane boundary, was determined from all flight data including the representative data of figure 14. The boundary decreases from the test limit normal-force coefficient at $M \approx 0.70$ to a normal-force coefficient of approximately 0.15 at $M = 0.95$.

CONCLUSIONS

The results obtained from wind-up turns performed over the Mach number range from 0.70 to 0.95 during flights of the NACA research

program of the Convair XF-92A airplane with and without wing fences indicate the following conclusions:

1. Over the Mach number range tested the airplane experienced a marked decrease in stability at moderate lift in the form of a pitch-up which appeared to be of an oscillatory nature. The region of reduced stability covered a relatively small angle-of-attack range and steady flight above and below this region was possible. A stability boundary that defines the normal-force coefficient where the stability becomes unsatisfactory was determined that decreased in normal-force coefficient from 0.40 to 0.15 as the Mach number increased from 0.70 to 0.95.

2. The longitudinal oscillation encountered in the region of reduced stability attained an amplitude of ± 1 g and had a period of about 2 seconds.

3. Excessive negative load factors were sometimes encountered during the recovery from pitch-ups as a result of the low damping, high control effectiveness, and poor characteristics of the hydraulic control system.

4. The speed loss during the maneuvers between Mach numbers of 0.80 and 0.90 could cause an incremental change in load factor in excess of 1 g with the controls fixed as a result of speed stability characteristics. This speed instability was felt by the pilots to be easily controllable.

5. There was no apparent pitch-up in the usable lift range at the lower Mach numbers with the wing fences installed. The improvement derived from the fences decreased with an increase in Mach number until no difference in stability characteristics could be noted between the fence configurations and the basic airplane at Mach numbers above approximately 0.90. No appreciable difference in stability characteristics was noted between the two fence configurations tested.

High-Speed Flight Station,
National Advisory Committee for Aeronautics,
Edwards, Calif., October 6, 1954.

[redacted]

APPENDIX

The static pitching-moment-coefficient variations presented in figures 8 and 15 were estimated from the flight data by using the basic moment equation:

$$C_m' = \frac{I_Y \ddot{\theta}}{qS\bar{c}}$$

where

$$C_m' = C_m + C_{m_{\delta_e}}\left(\delta_e - \delta_{e_1}\right) + C_{m_{\dot{\theta}}} \frac{\dot{\theta}\bar{c}}{2V} + C_{m_{\dot{\alpha}}} \frac{\dot{\alpha}\bar{c}}{2V}$$

The damping in pitch of the tailless XF-92A airplane is small and neglecting the damping terms was found to have only a small effect on the calculated results. Neglecting the damping terms simplifies the preceding equation to:

$$C_m = \frac{I_Y \ddot{\theta}}{qS\bar{c}} - C_{m_{\delta_e}}\left(\delta_e - \delta_{e_1}\right)$$

Unpublished flight test data indicated a value of $C_{m_{\delta_e}} = -0.01$ that was essentially constant with Mach number in the flight test range. Although the variation with lift is unknown, the data of reference 6 indicate that the control effectiveness should be very nearly constant to angles of attack of the order of 15° to 20°. It appears unlikely, however, that the value of $C_{m_{\delta_e}}$ would be unaffected by the separation and flow disturbances which probably cause the pitching-moment nonlinearities. In addition, the installation of fences would probably affect $C_{m_{\delta_e}}$. The physical characteristics used in the computations are listed in table I. Reference 7 gives a more detailed development and application of this type of analysis.

REFERENCES

1. Sisk, Thomas R., and Mooney, John M.: Preliminary Measurements of Static Longitudinal Stability and Trim for the XF-92A Delta-Wing Research Airplane in Subsonic and Transonic Flight. NACA RM L53B06, 1953.

2. Holleman, Euclid C., Evans, John H., and Triplett, William C.: Preliminary Flight Measurements of the Dynamic Longitudinal Stability Characteristics of the Convair XF-92A Delta-Wing Airplane. NACA RM L53E14, 1953.

3. Zalovcik, John A.: A Radar Method of Calibrating Airspeed Installations on Airplanes in Maneuvers at High Altitudes and at Transonic and Supersonic Speeds. NACA Rep. 985, 1950. (Supersedes NACA TN 1979.)

4. Finch, Thomas W., and Walker, Joseph A.: Flight Determination of the Static Longitudinal Stability Boundaries of the Bell X-5 Research Airplane with 59° Sweepback. NACA RM L53A09b, 1953.

5. Anderson, Seth B., and Bray, Richard S.: A Flight Evaluation of the Longitudinal Stability Characteristics Associated With the Pitch-Up of a Swept-Wing Airplane in Maneuvering Flight at Transonic Speeds. NACA RM A51I12, 1951.

6. Stephenson, Jack D., and Amuedo, Arthur R.: Tests of a Triangular Wing of Aspect Ratio 2 in the Ames 12-Foot Pressure Wind Tunnel. II - The Effectiveness and Hinge Moments of a Constant-Chord Flap. NACA RM A8E03, 1948.

7. Campbell, George S., and Weil, Joseph: The Interpretation of Nonlinear Pitching Moments in Relation to the Pitch-Up Problem. NACA RM L53I02, 1953.

TABLE I

PHYSICAL CHARACTERISTICS OF THE XF-92A AIRPLANE

Wing:	
Area, sq ft	425
Span, ft	31.33
Airfoil section	NACA 65(06)-006.5
Mean aerodynamic chord, ft	18.09
Aspect ratio	2.31
Root chord, ft	27.13
Tip chord	0
Taper ratio	0
Sweepback (leading edge), deg	60
Incidence, deg	0
Dihedral (chord plane), deg	0
Elevons:	
Area (total of both elevons aft of hinge line), sq ft	76.19
Horn balance area (total of both elevons forward of hinge line), sq ft	1.4
Span (one elevon), ft	13.35
Chord (aft of hinge line, constant except at tip), ft	3.05
Movement, deg	
Elevator:	
Up	15
Down	5
Aileron, total	10
Operation	Hydraulic
Vertical tail:	
Area, sq ft	75.35
Height, above fuselage center line, ft	11.50
Rudder:	
Area, sq ft	15.53
Span, ft	9.22
Travel, deg	±8.5
Operation	Hydraulic
Fuselage:	
Length, ft	42.80
Power plant:	
Engine	Allison J33-A-29 with afterburner
Rating:	
Static thrust at sea level, lb	5,600
Static thrust at sea level with afterburner, lb	7,500
Weight:	
Gross weight (560 gal fuel), lb	15,560
Empty weight, lb	11,808
Center-of-gravity locations:	
Gross weight (560 gal fuel), percent M.A.C.	25.5
Empty weight, percent M.A.C.	29.2
Moment of inertia in pitch, slug-ft^2	35,000

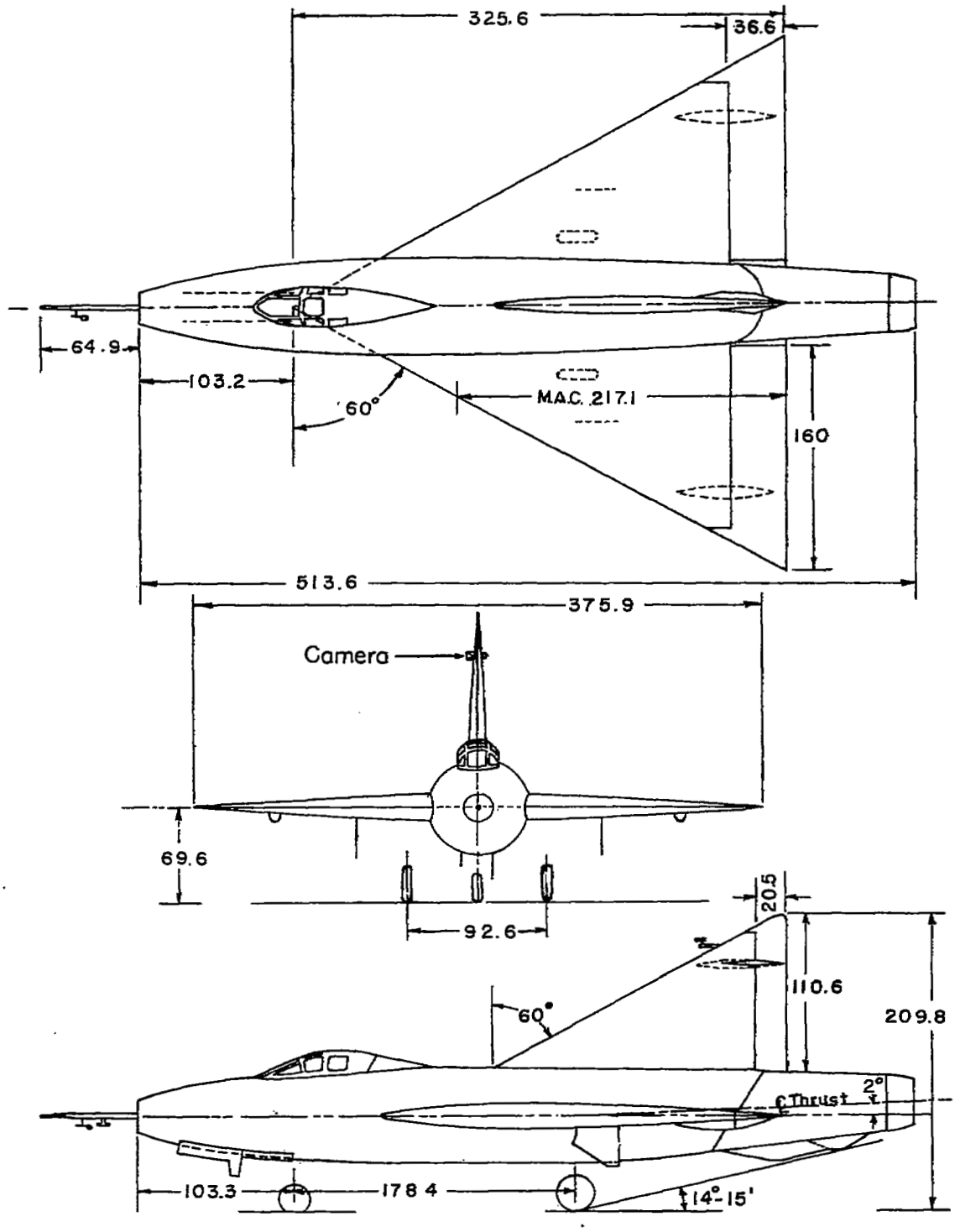

Figure 1.- Three-view drawing of the XF-92A airplane. (All dimensions in inches.)

[redacted]

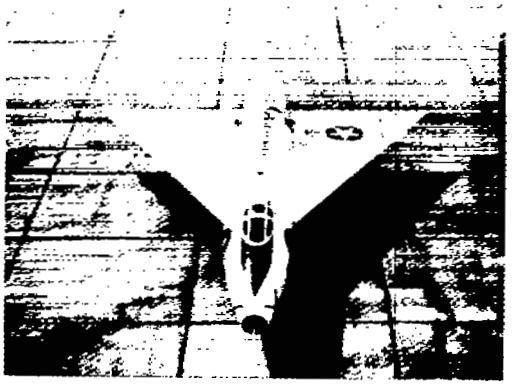

(a) Overhead front view.

(b) Three-quarter rear view.

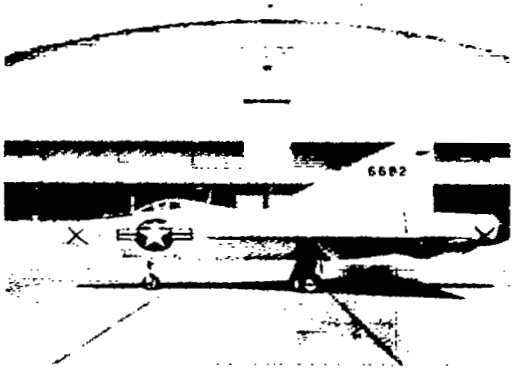

(c) Left side view.

L-81260

Figure 2.- Photograph of the XF-92A airplane.

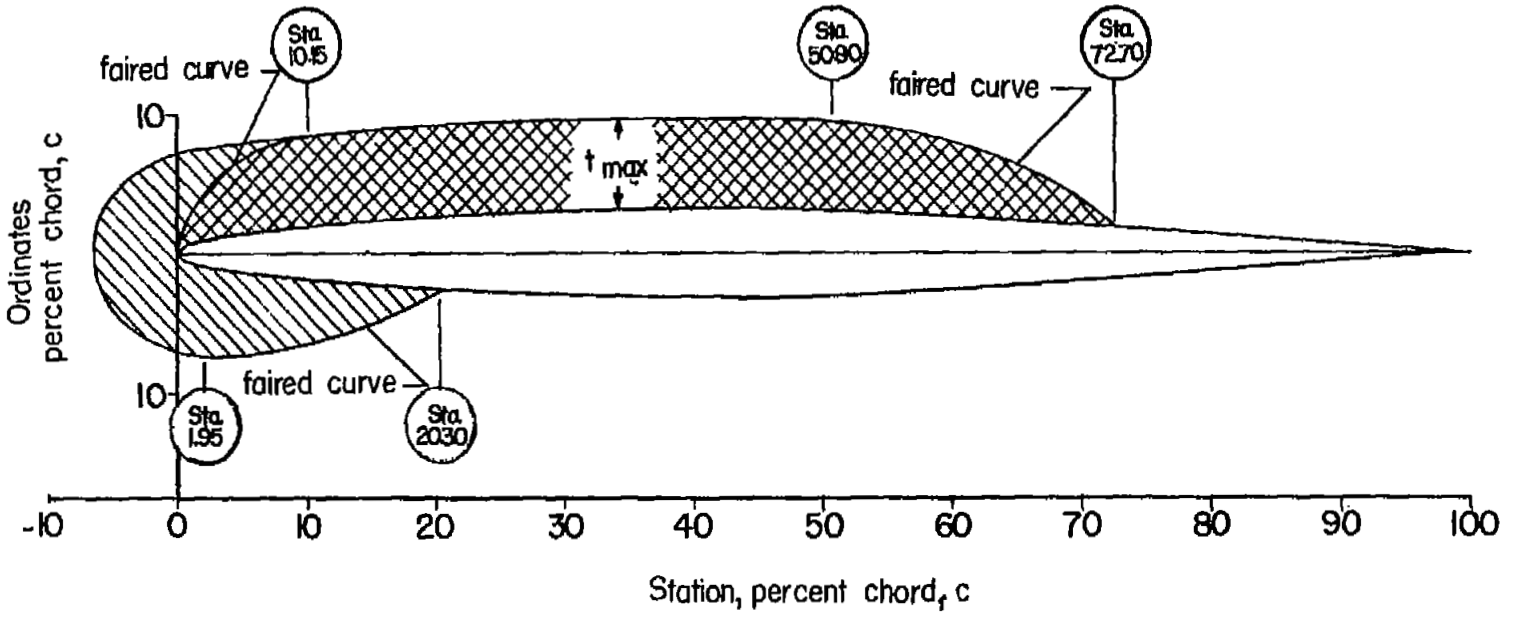

Basic fence
Modified fence
Fence located at 0.607 wing semispan (114.10 in.)
Wing chord at fence station = 127.94 in.
Maximum wing thickness at fence station = 8.32 in.

Figure 3.- Wing fence configuration.

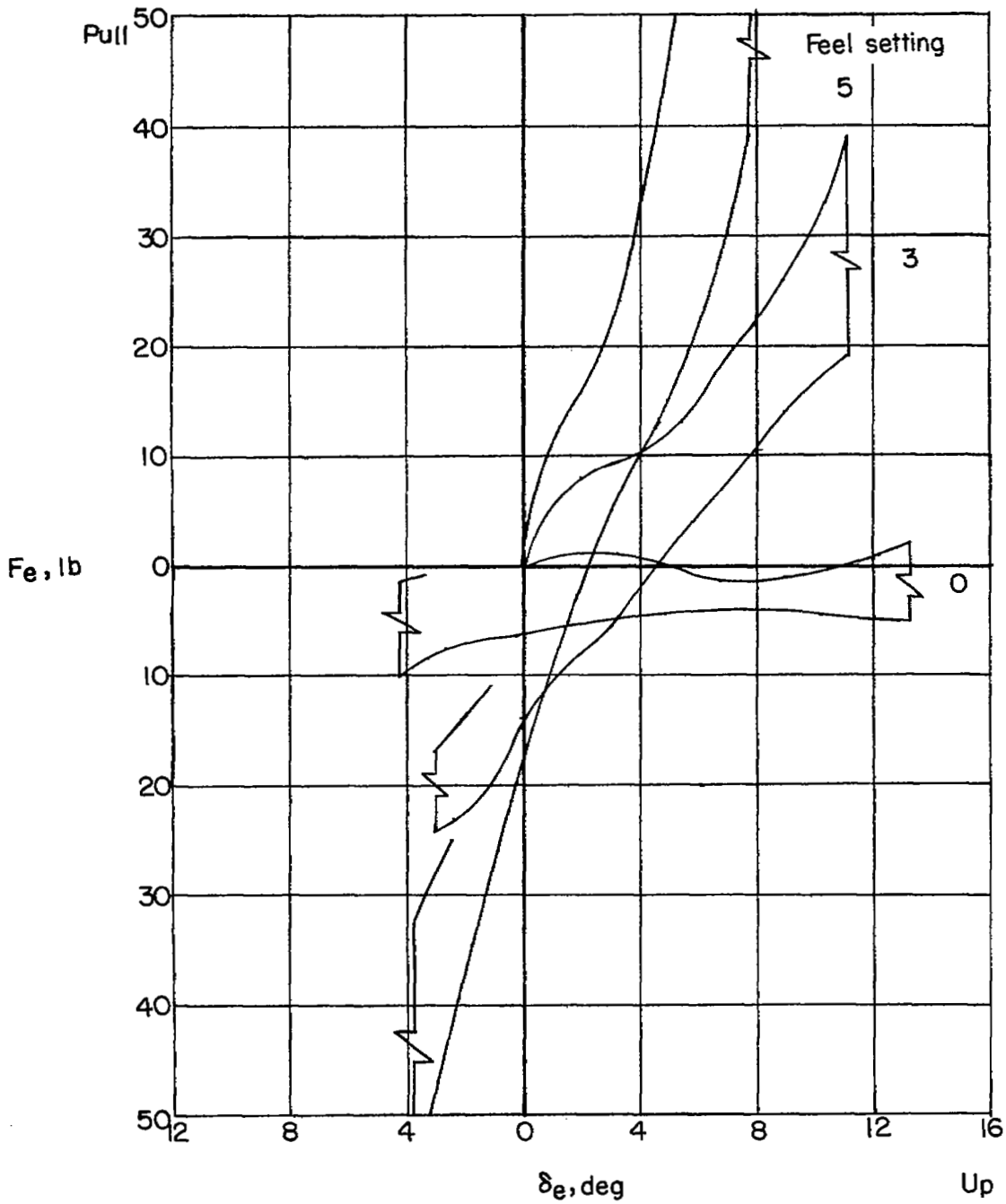

(a) Variation of stick force with elevon angle for three feel settings.

Figure 4.- Ground and flight measurements of the characteristics of the XF-92A longitudinal control and feel system.

[redacted]

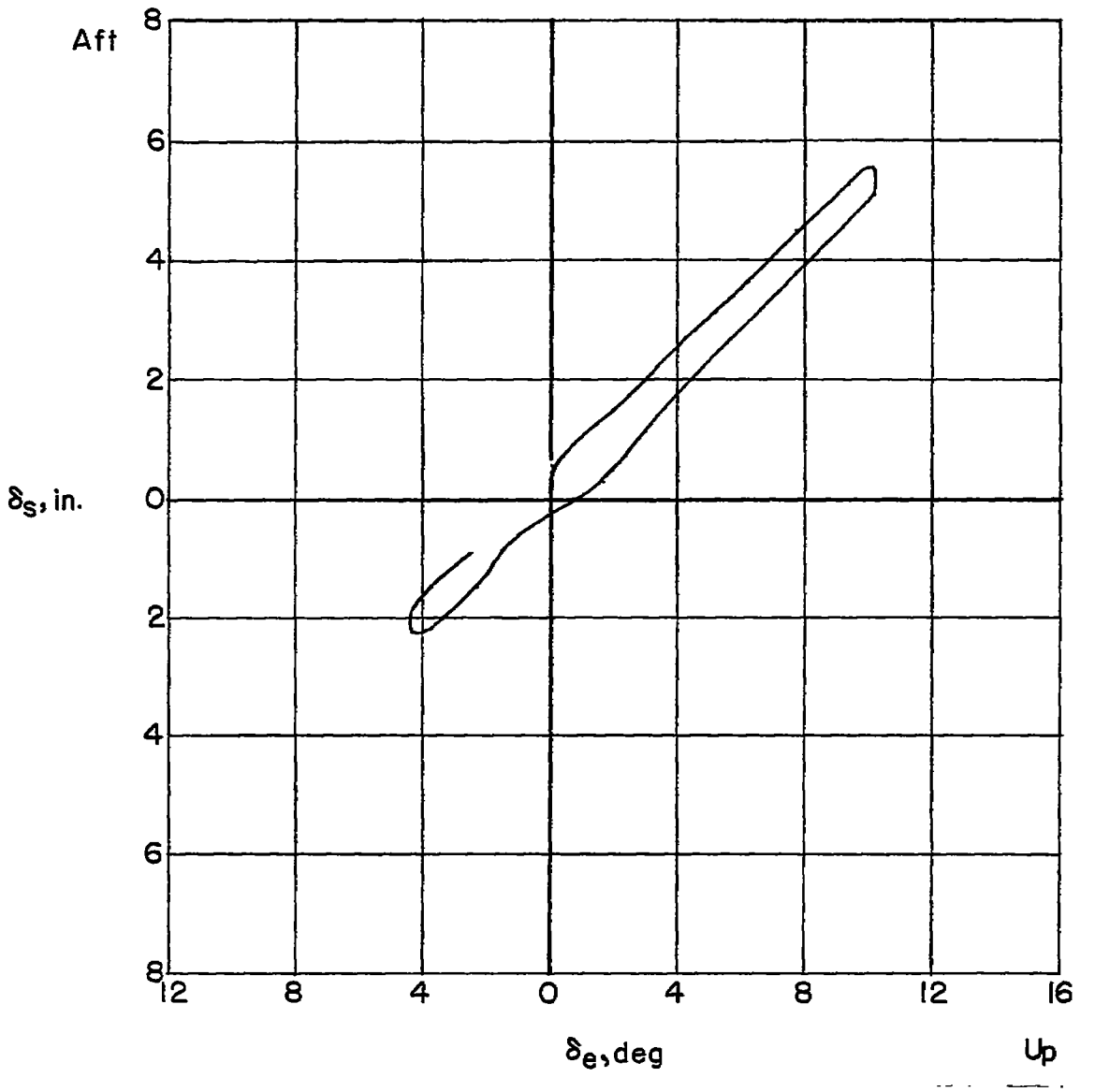

(b) Variation of stick position with elevon angle.

Figure 4.- Continued.

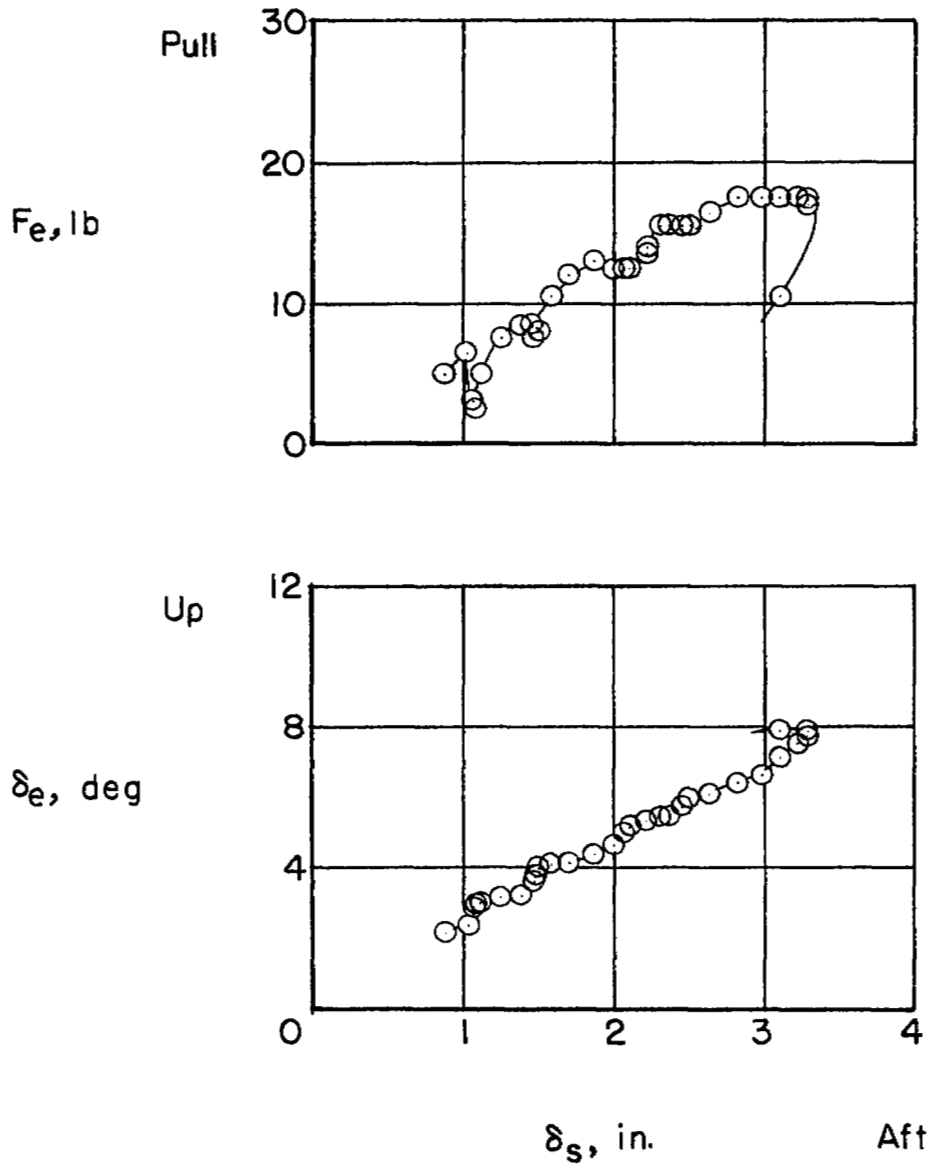

(c) Variation of longitudinal stick force and elevon angle with longitudinal stick position as obtained in a flight maneuver.

Figure 4.- Concluded.

[redacted]

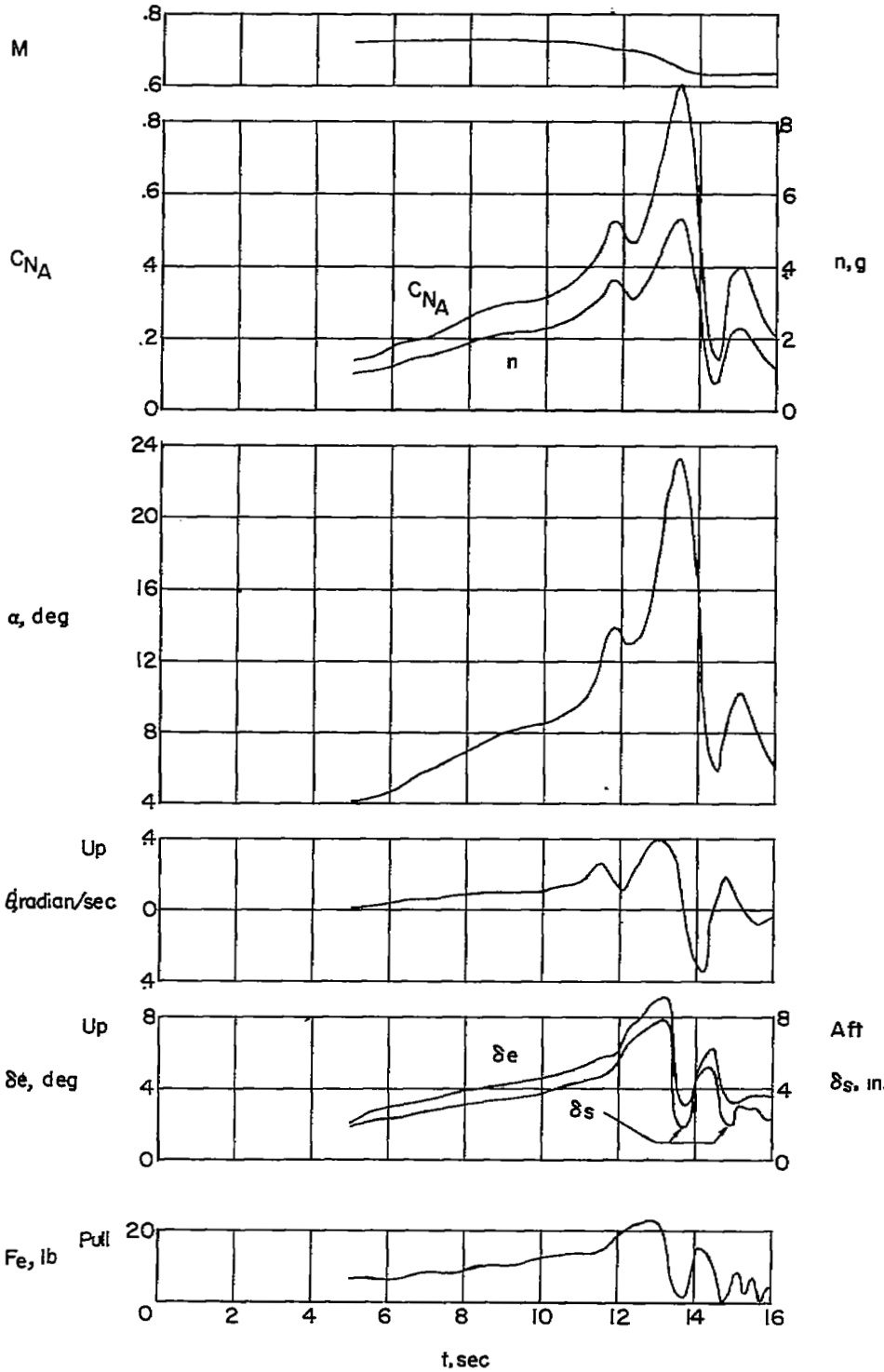

Figure 5.- Example of normal wind-up turn for XF-92A initiated at M = 0.72.

[redacted]

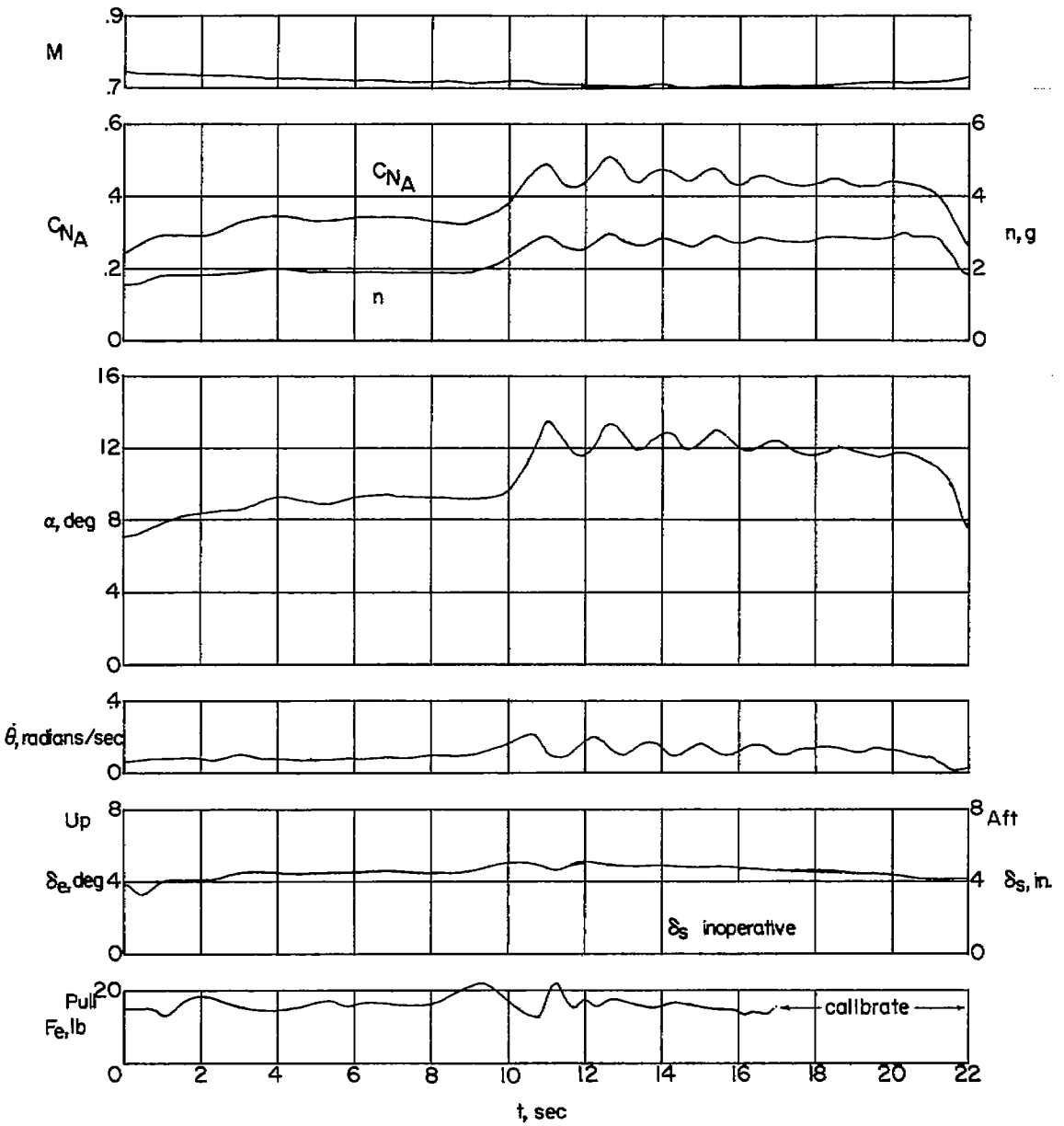

(a) $M \approx 0.70$; $n \approx 2.0g$ and $3.0g$; $h_p = 33{,}500$ feet.

Figure 6.- Examples of constant-acceleration turns for XF-92A below and at stability change.

[redacted]

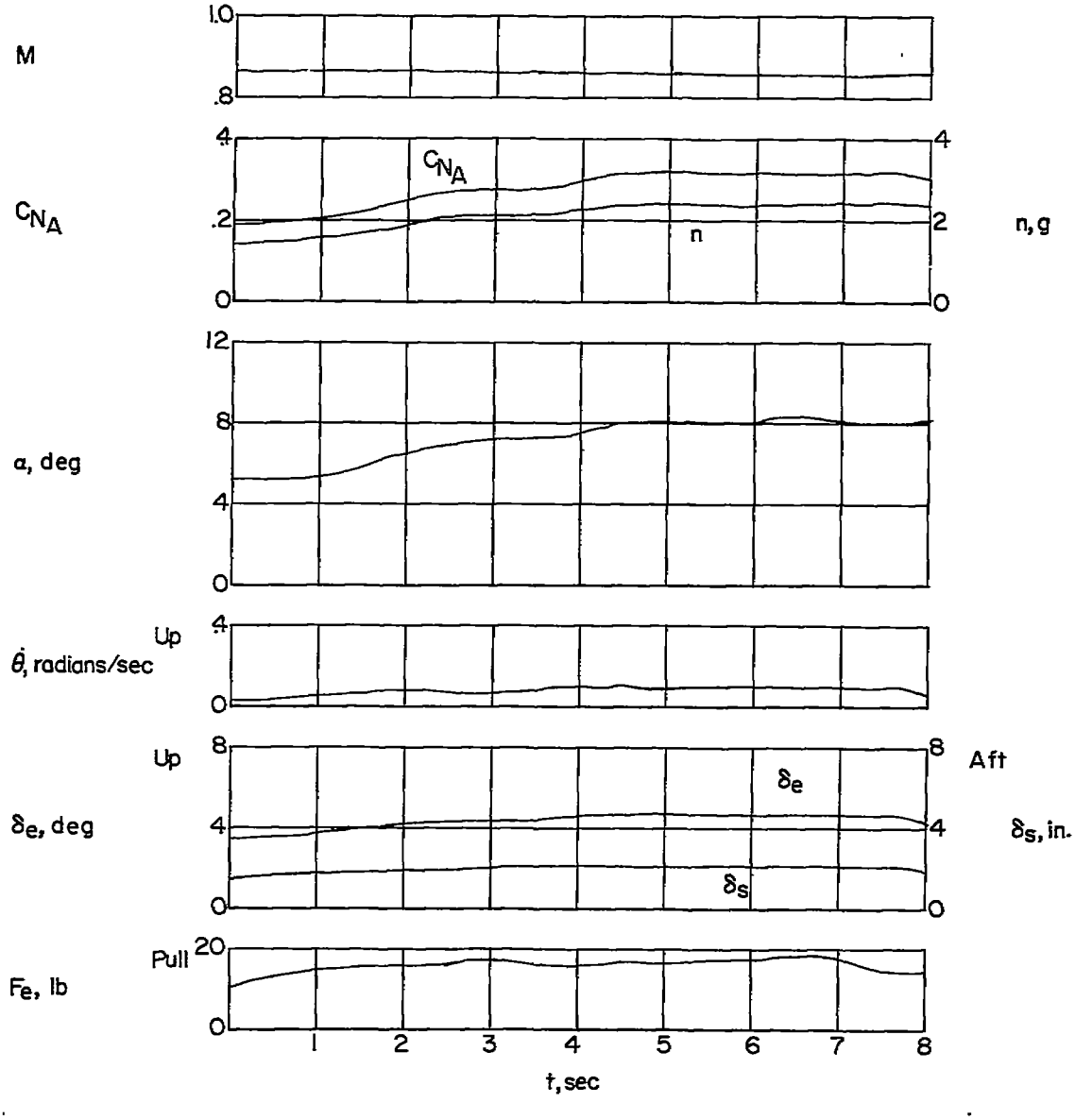

(b) $M \approx 0.85$; $n \approx 2.0g$; $h_p = 36,500$ feet.

Figure 6.- Continued.

[redacted]

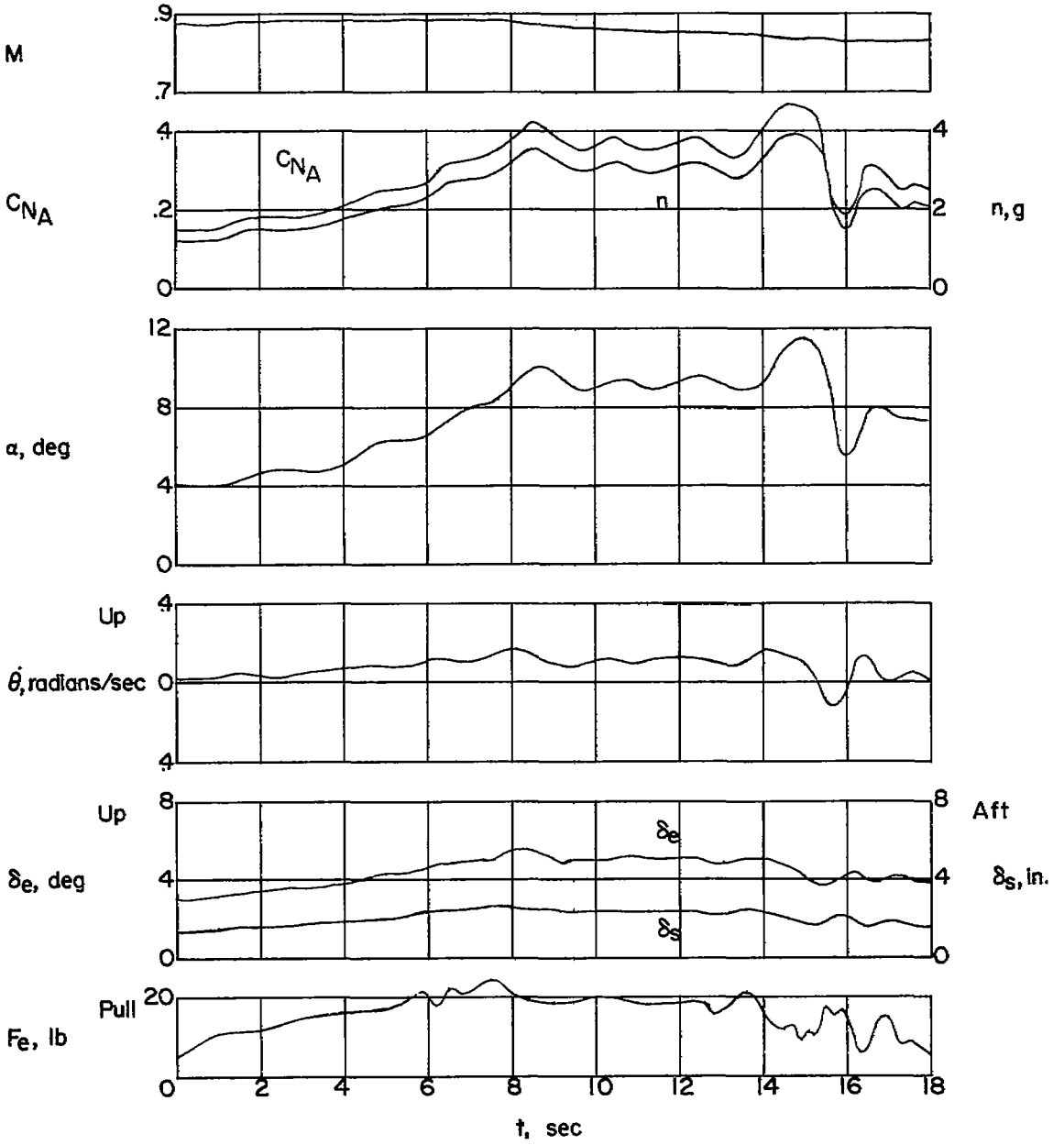

(c) $M \approx 0.85$; $n \approx 3.0g$; $h_p = 35{,}000$ feet.

Figure 6.- Concluded.

[redacted]

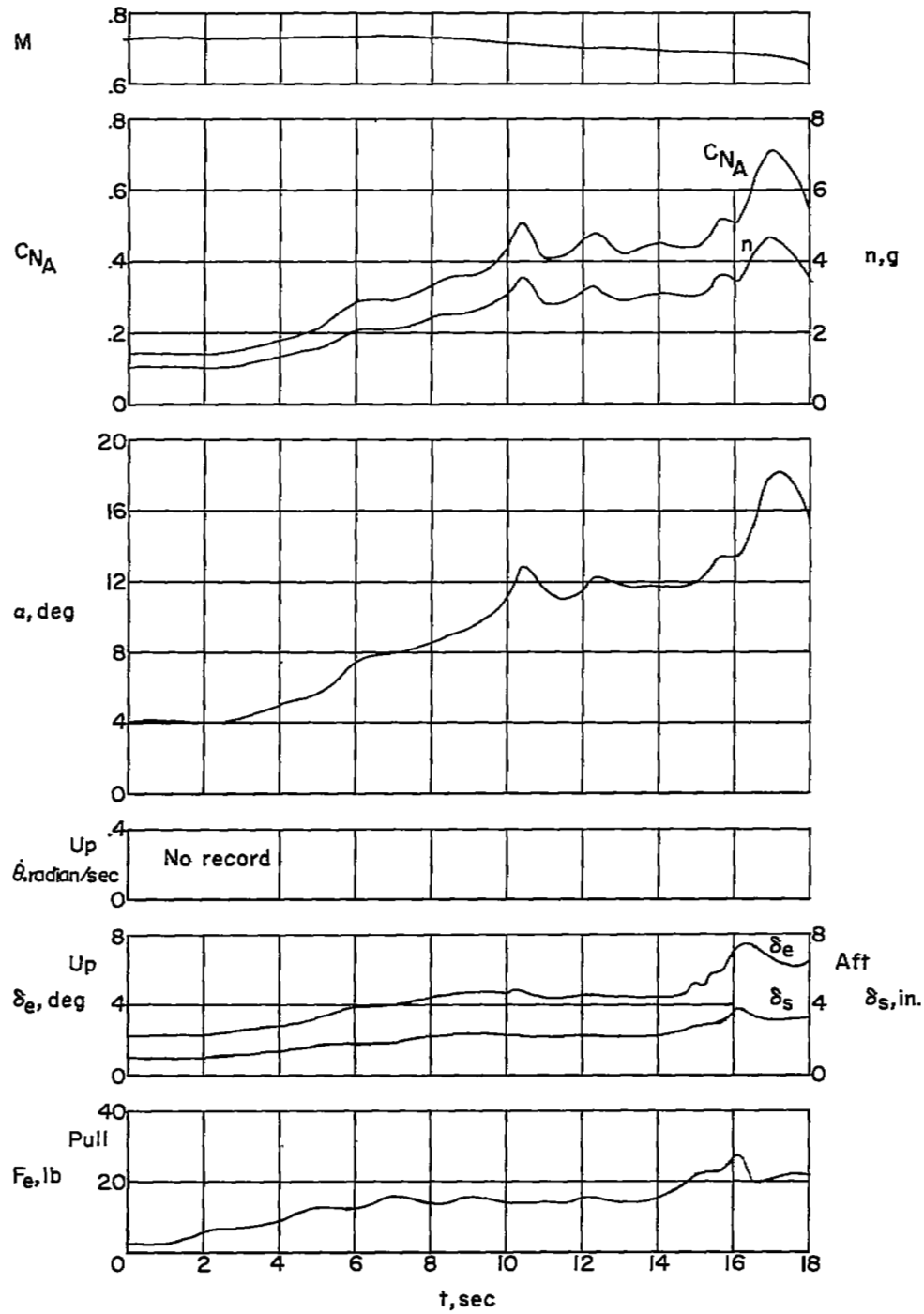

(a) $M \approx 0.70$; $h_p = 31,500$ feet.

Figure 7.- Representative time histories of wind-up turns for XF-92A.

[redacted]

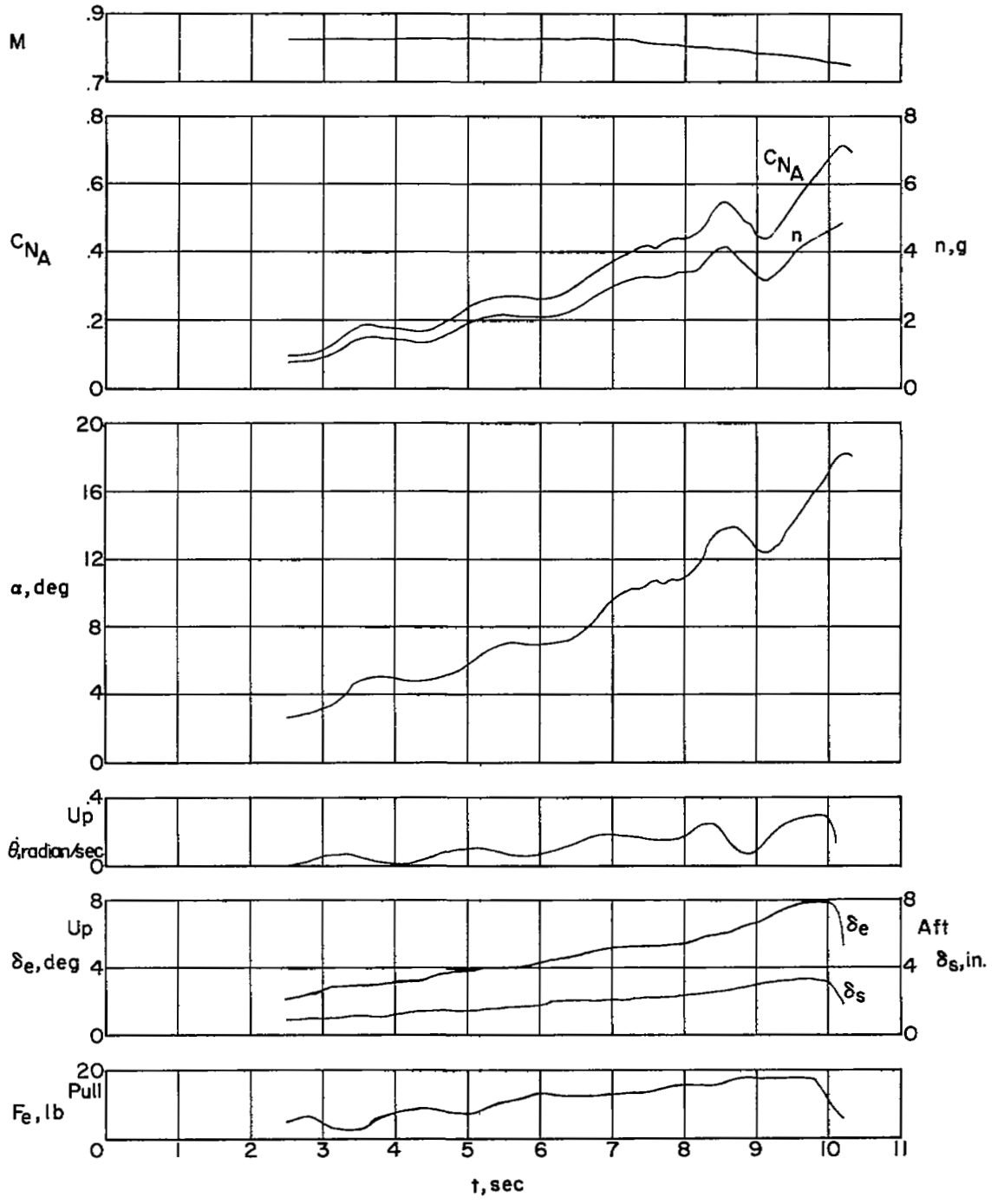

(b) $M \approx 0.80$; $h_p = 33{,}600$ feet.

Figure 7.- Continued.

[redacted]

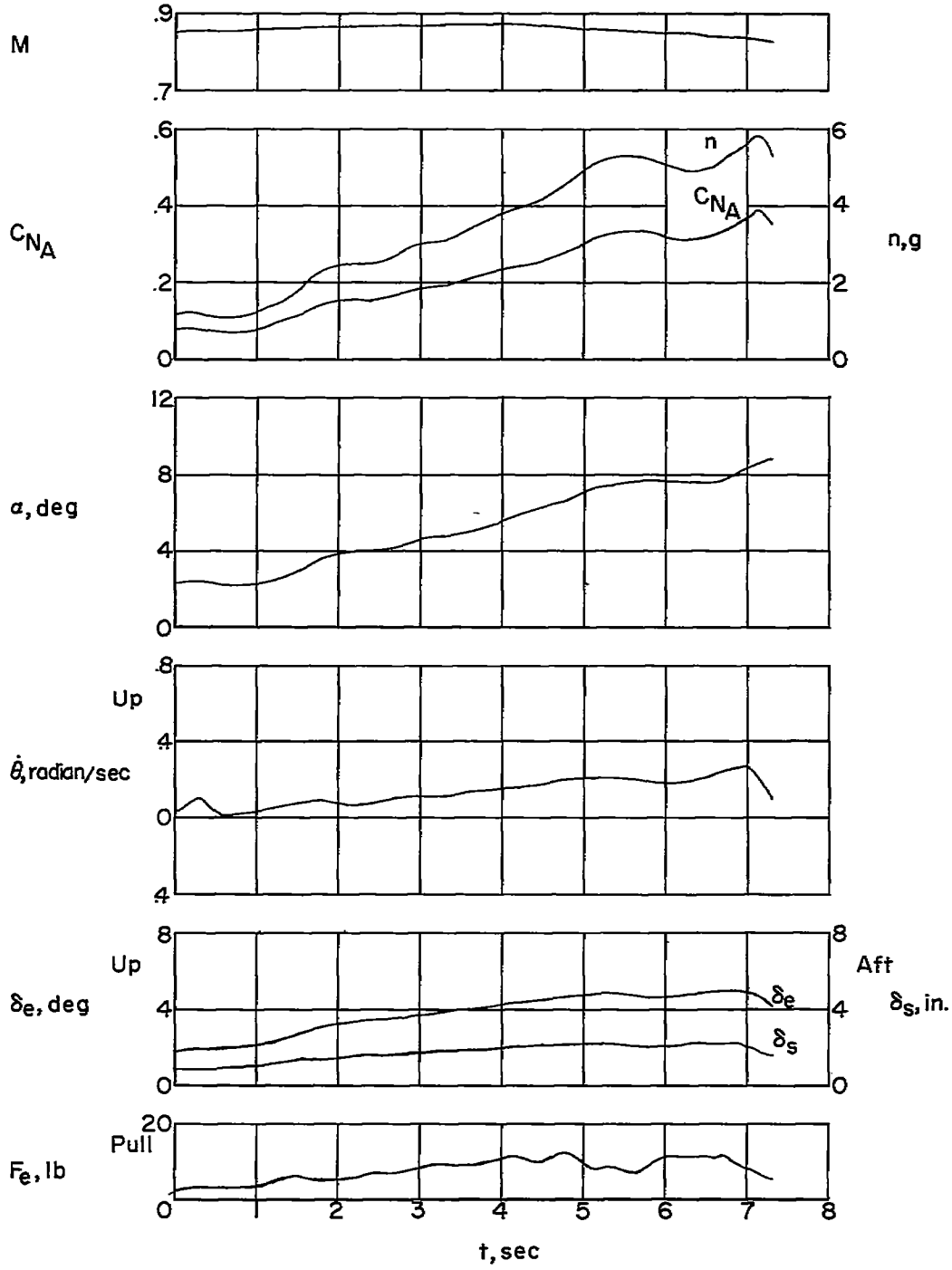

(c) $M \approx 0.85$; $h_p = 21{,}700$ feet.

Figure 7.- Continued.

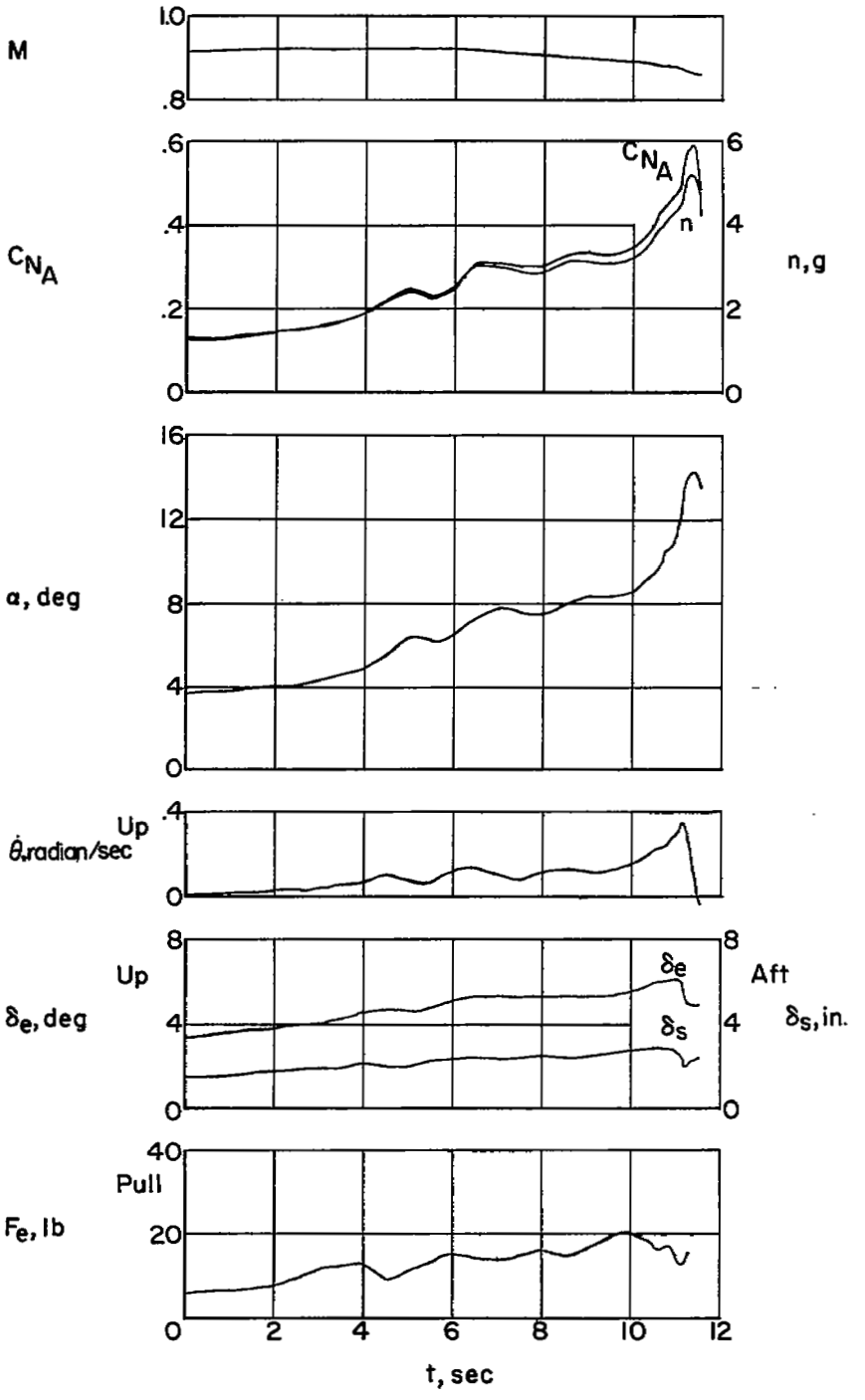

(d) $M \approx 0.90$; $h_p = 35{,}200$ feet.

Figure 7.- Continued.

[redacted]

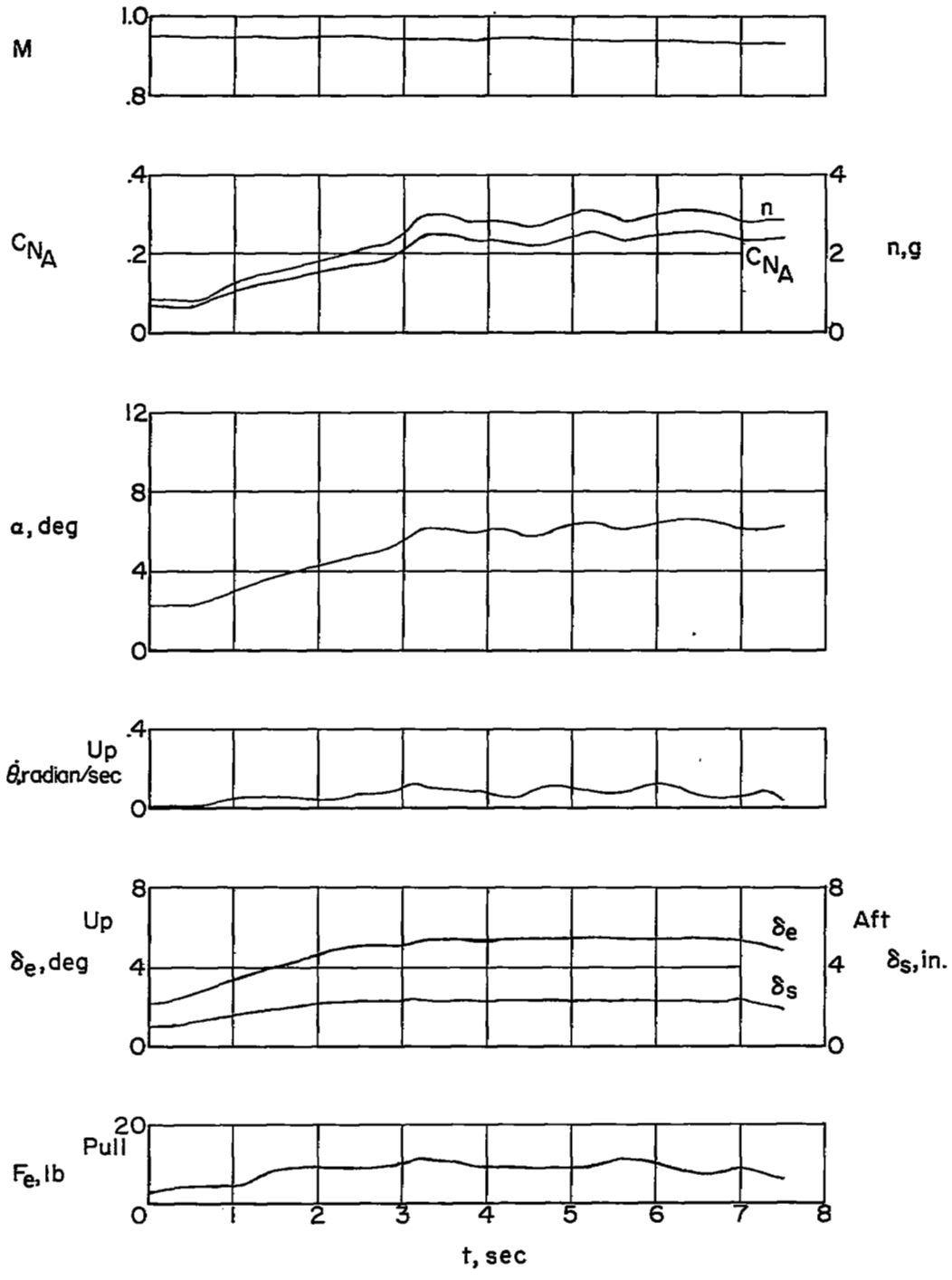

(e) $M \approx 0.95$; $h_p = 31{,}500$ feet.

Figure 7.- Concluded.

[redacted]

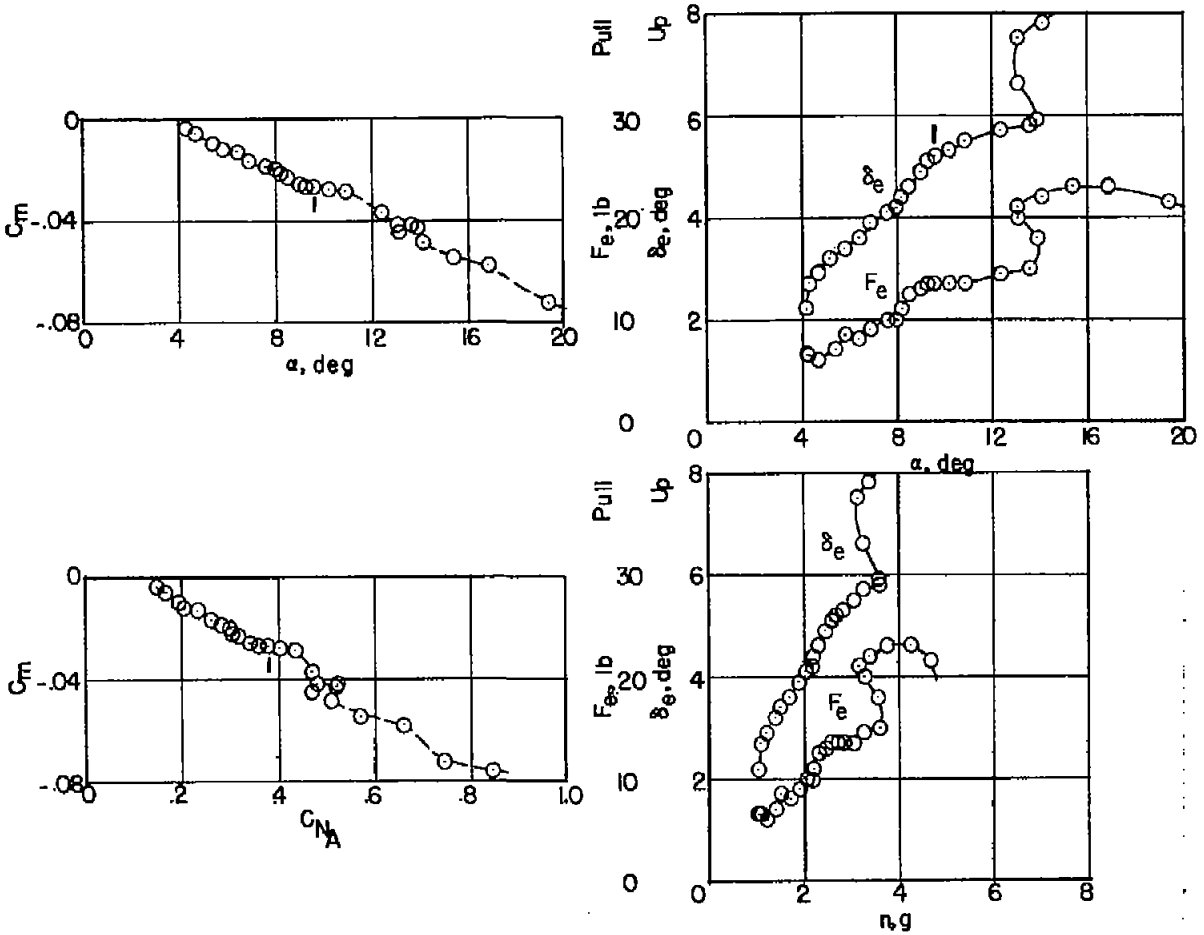

(a) M ≈ 0.70.

Figure 8.- Maneuvering stability characteristics of the XF-92A airplane at various Mach numbers.

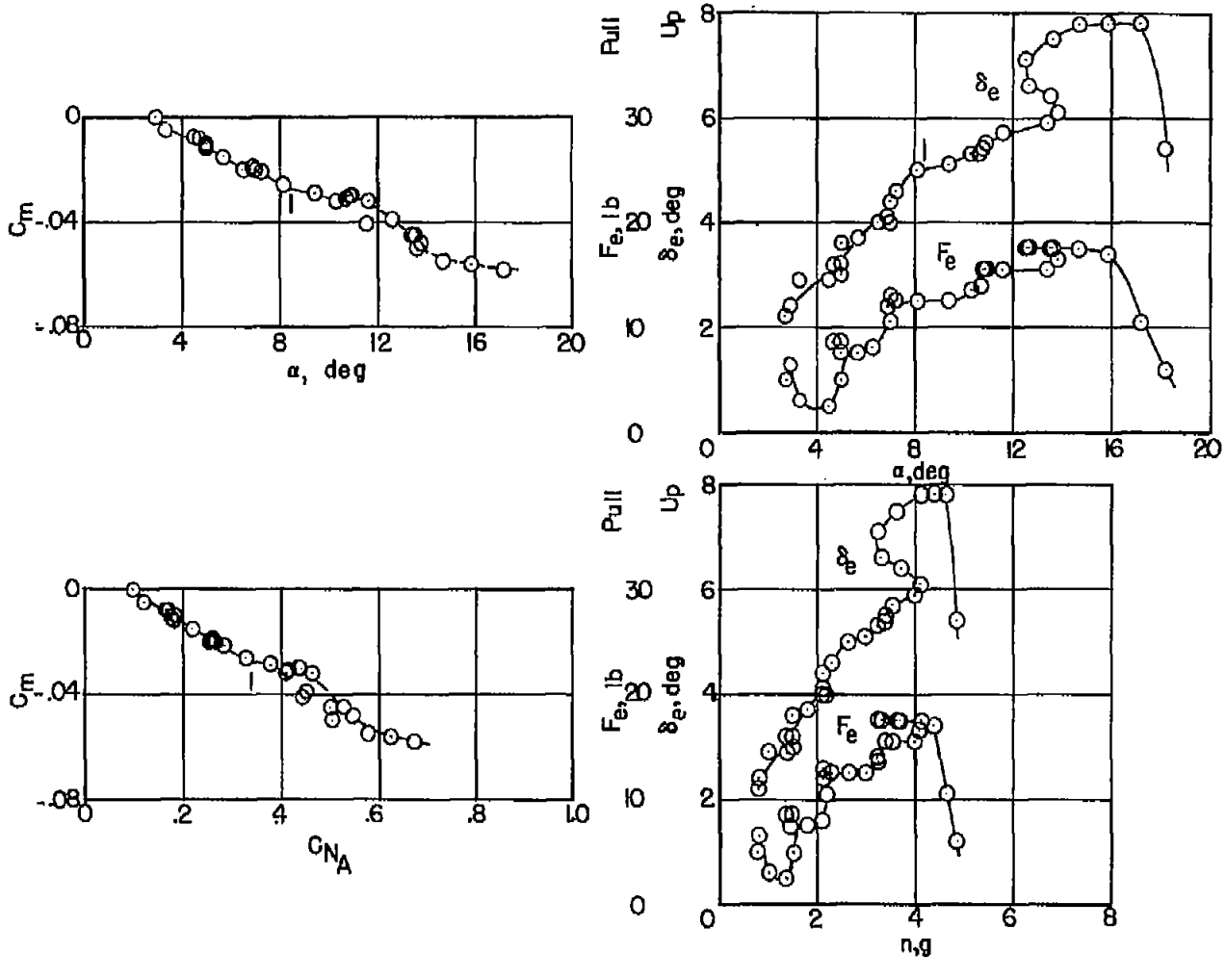

(b) $M \approx 0.80$.

Figure 8.- Continued.

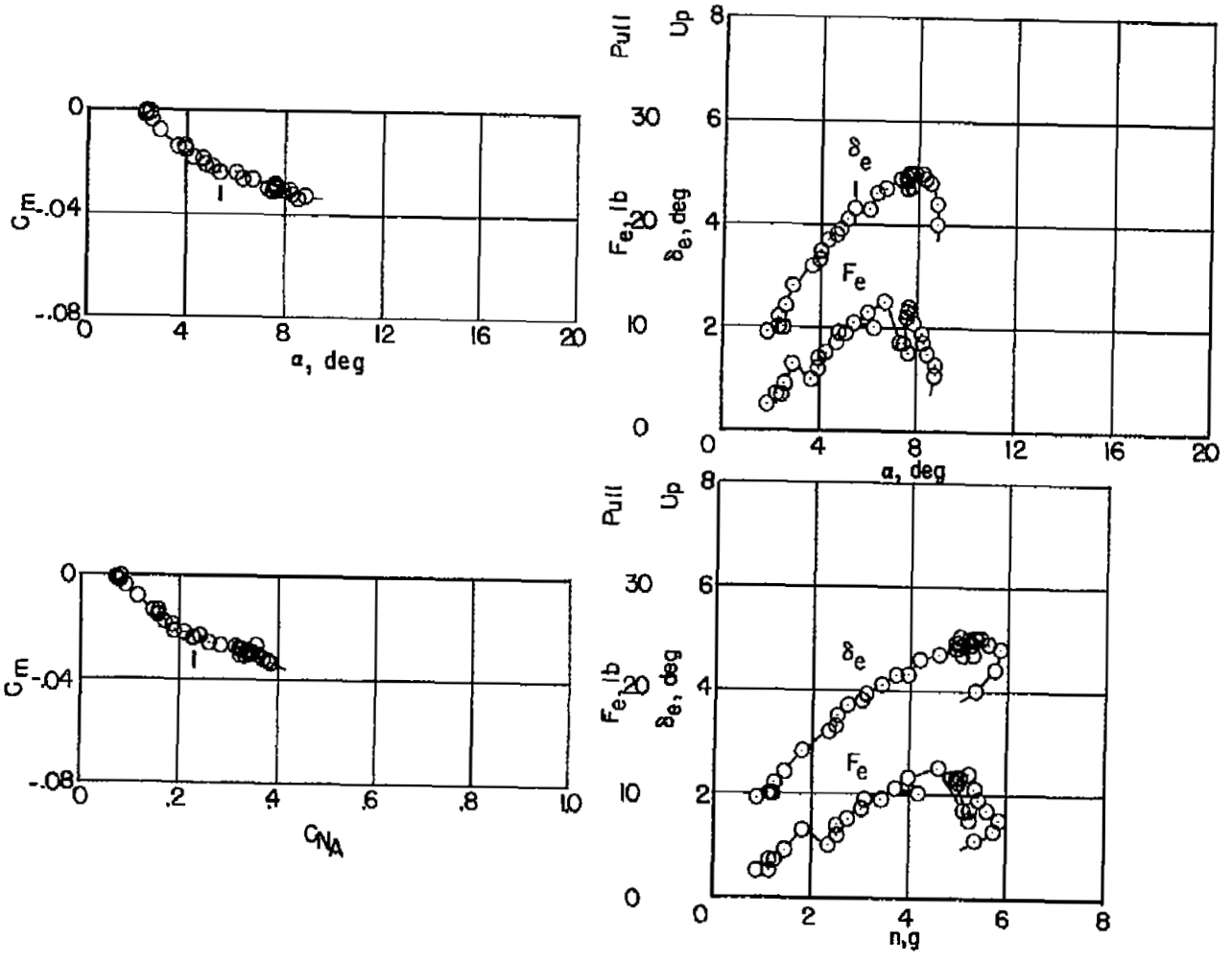

(c) $M \approx 0.85$.

Figure 8.- Continued.

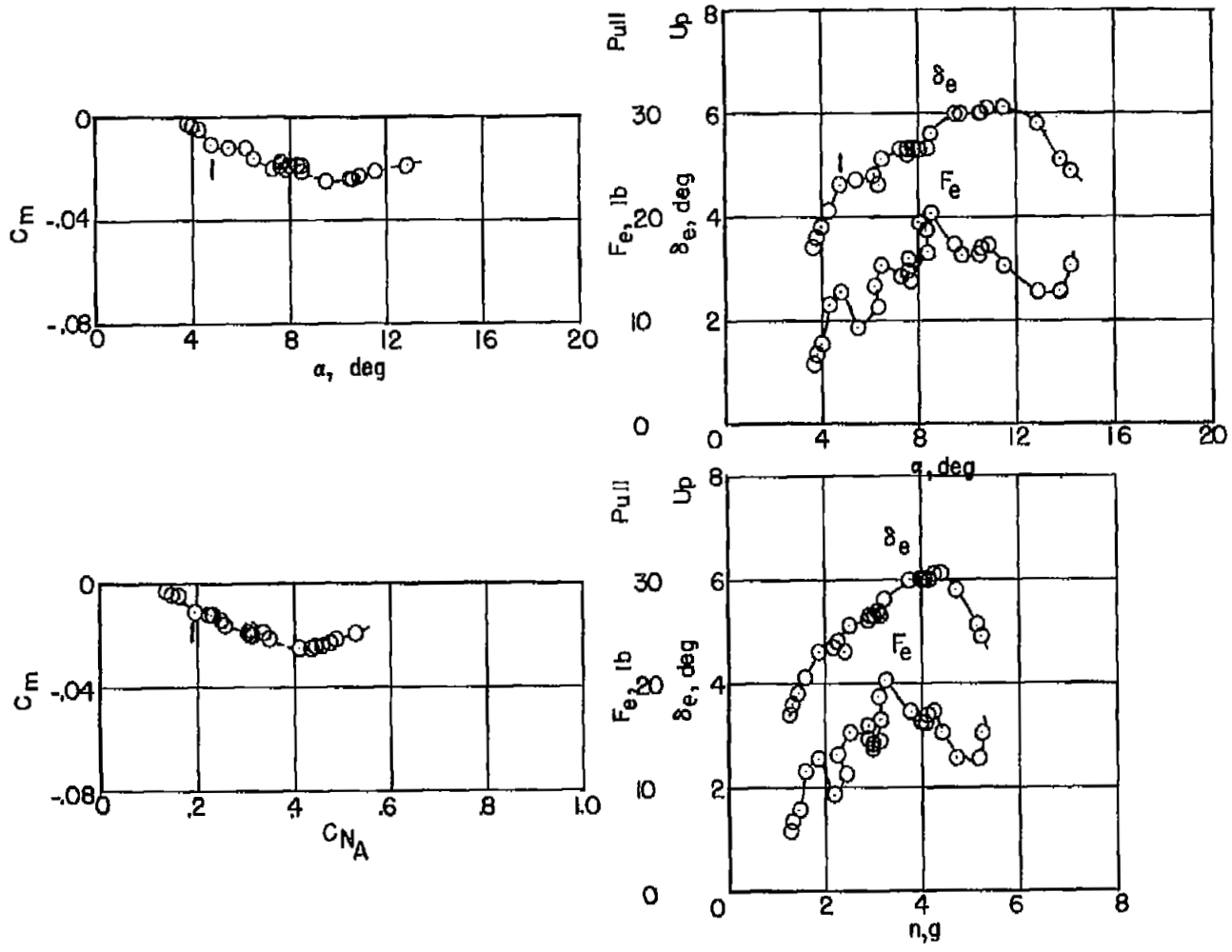

(d) $M \approx 0.90$.

Figure 8.- Continued.

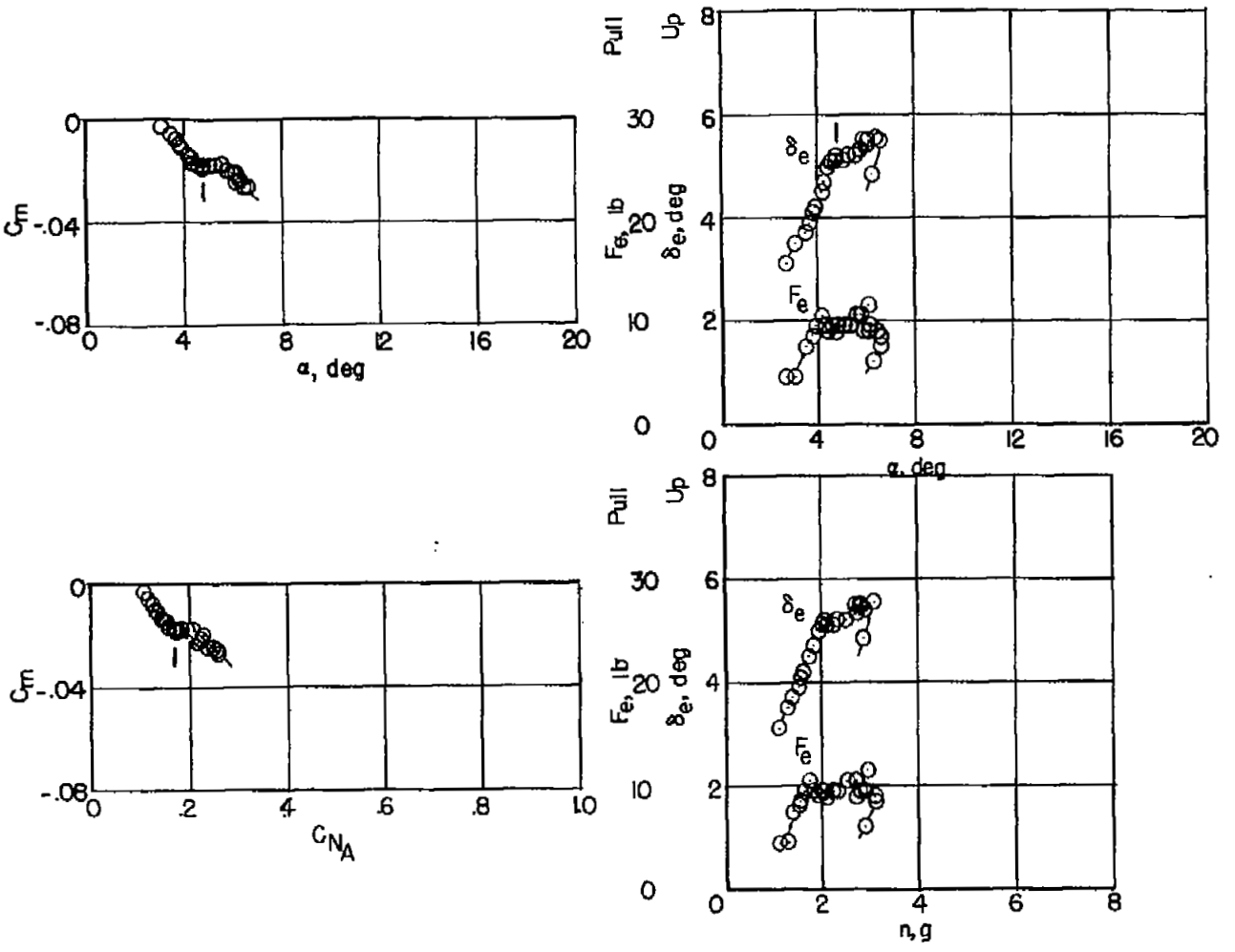

(e) $M \approx 0.95$.

Figure 8.- Concluded.

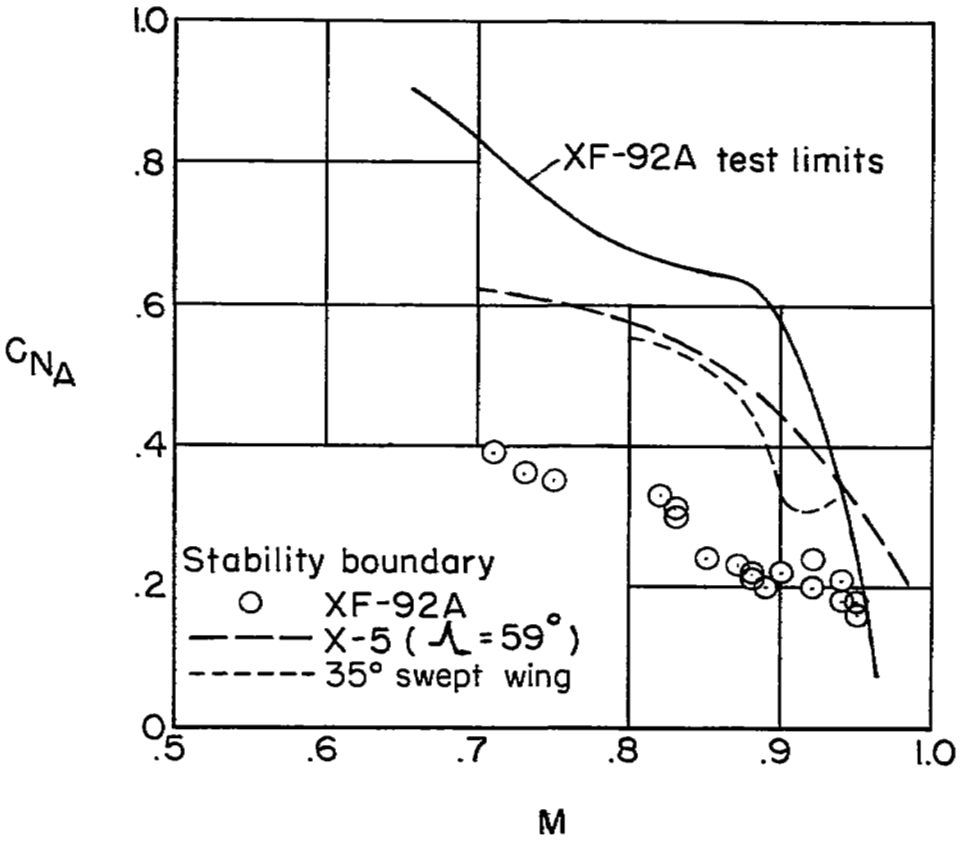

Figure 9.- Boundary for stability decay for the XF-92A and comparison with other configurations.

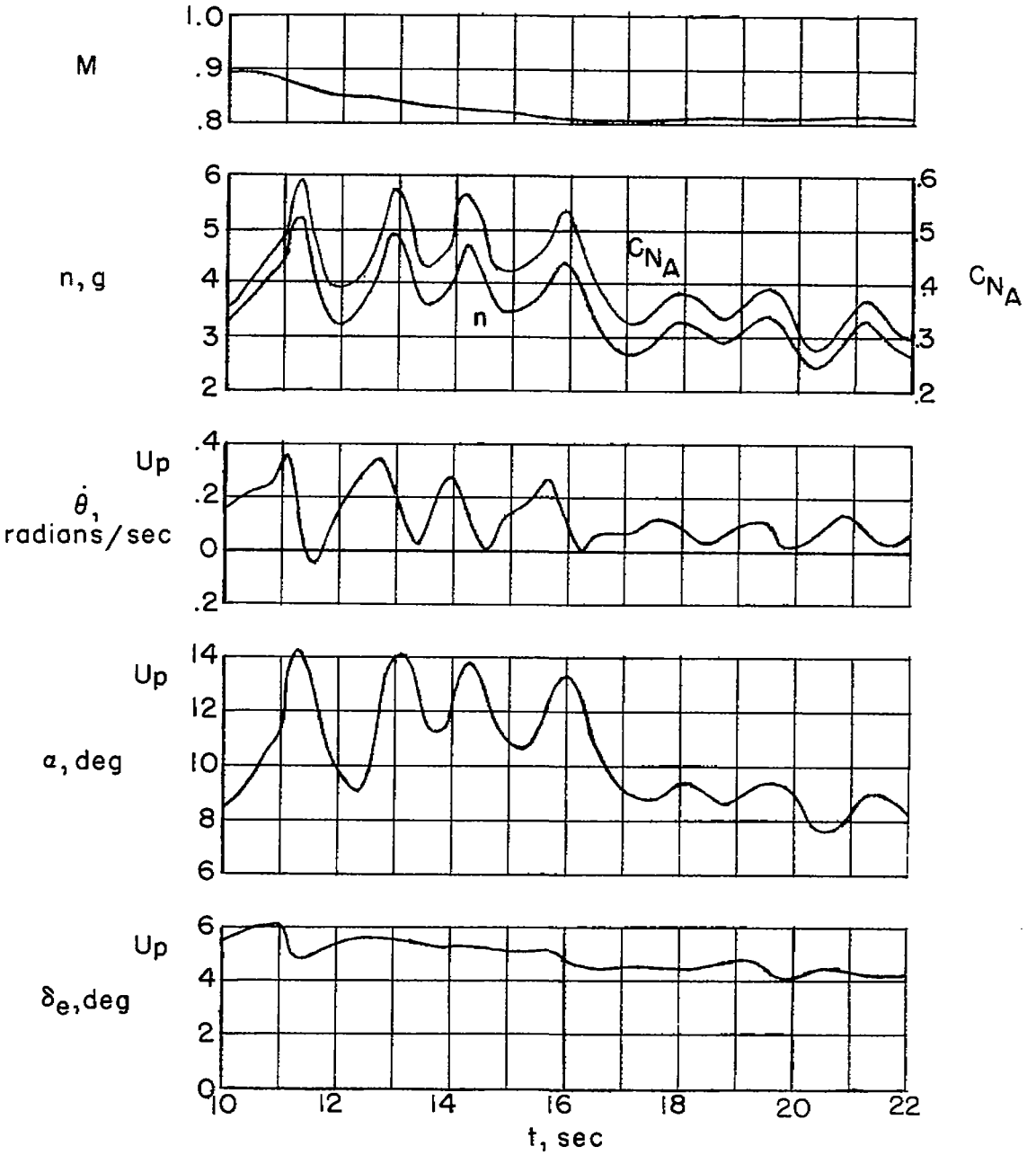

Figure 10.- Pitching oscillations encountered at moderate lift coefficient. h_p = 34,500 feet.

[redacted]

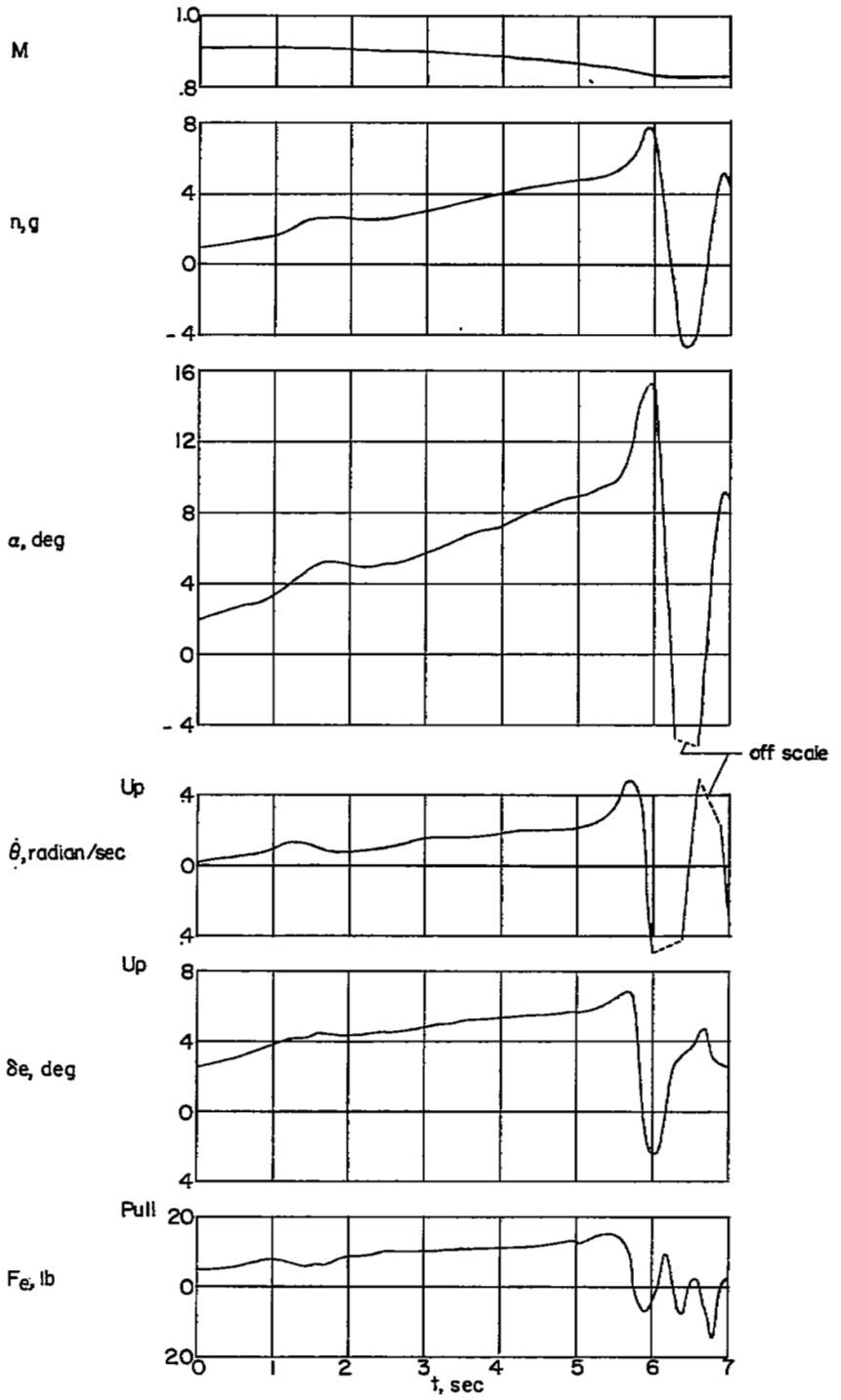

Figure 11.- Wind-up turn for XF-92A in which a large negative load factor was encountered during the recovery. h_p = 26,200 feet.

[redacted]

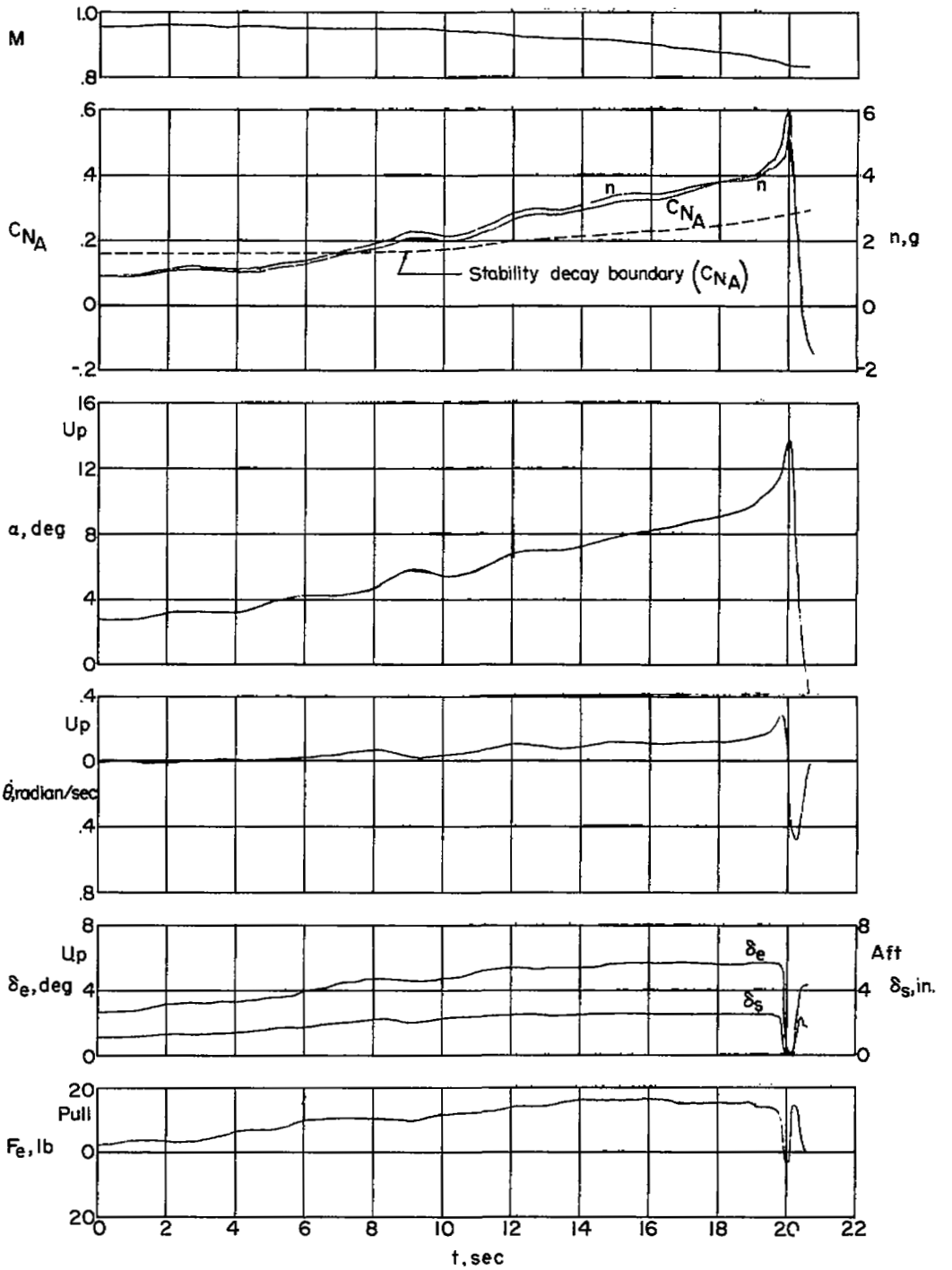

Figure 12.- Wind-up turn for XF-92A showing steady flight above the boundary for stability decay. h_p = 34,700 feet.

[redacted]

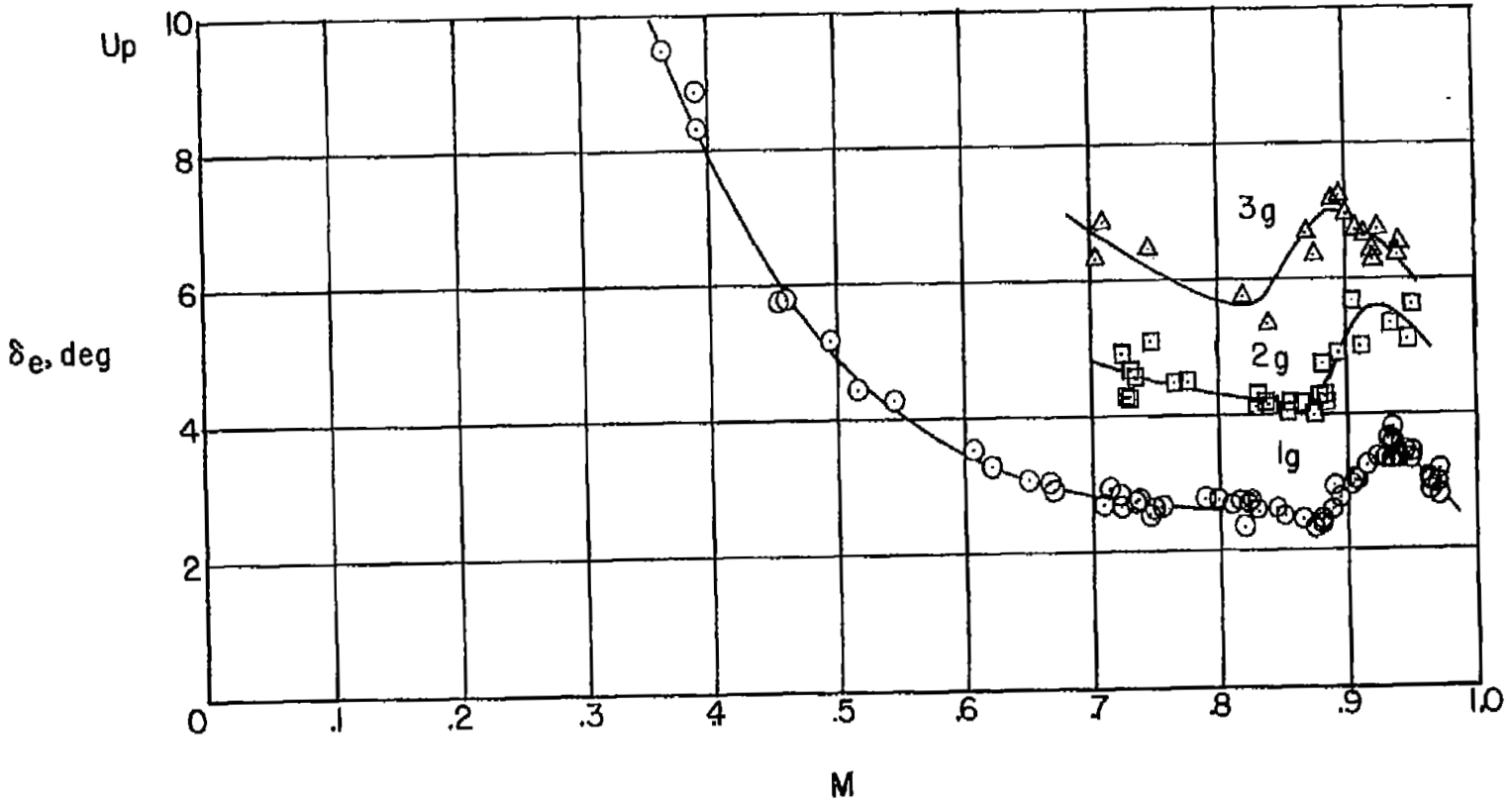

Figure 13.- Variation of longitudinal control angle with Mach number for 1.0g, 2.0g, and 3.0g corrected to 35,000 feet altitude. (c.g. = 27.2 to 28.7 percent M.A.C.)

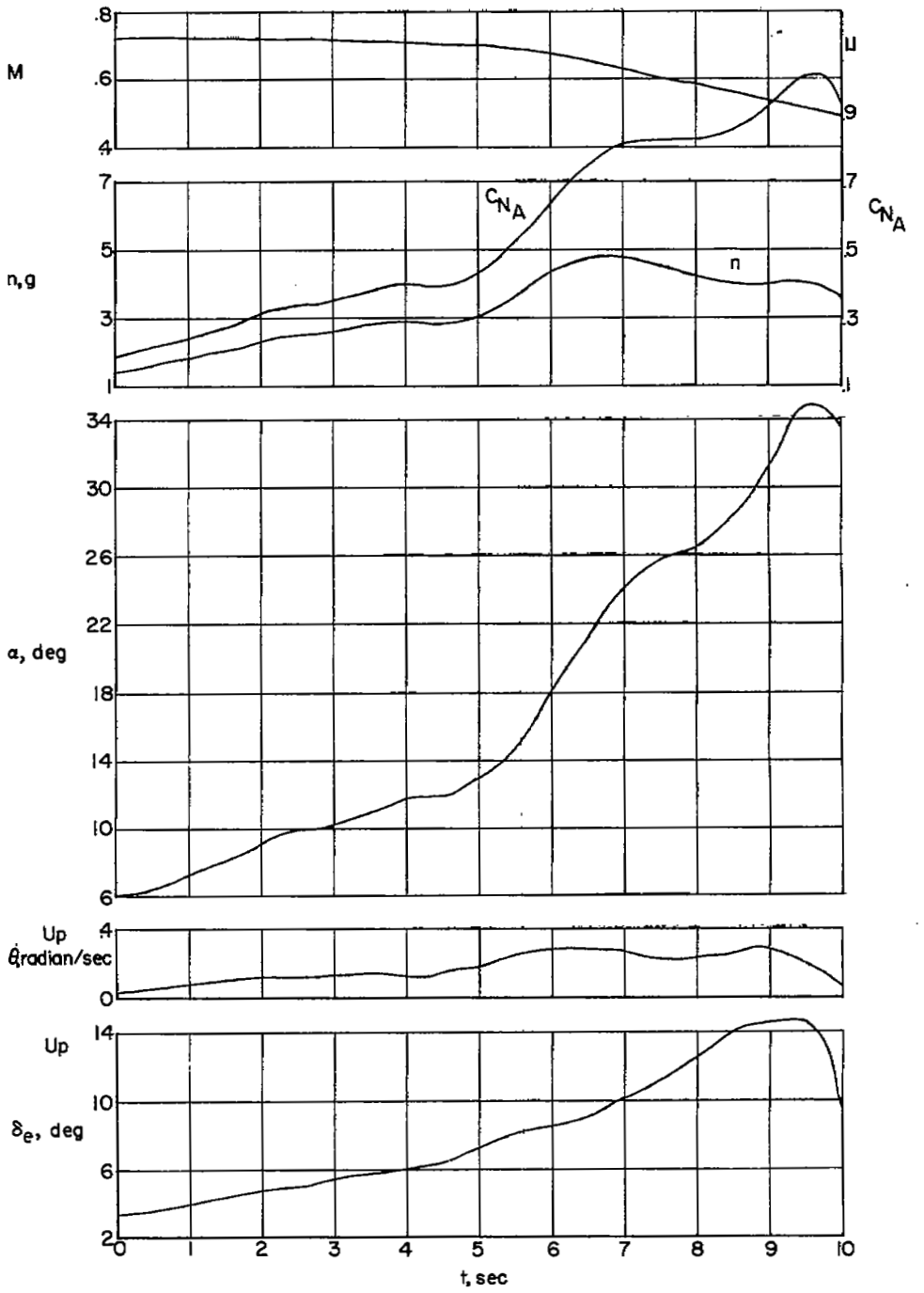

(a) $M \approx 0.70$; h_p = 29,900 feet; basic fence configuration.

Figure 14.- Representative time histories of wind-up turns for XF-92A with wing fences installed.

[redacted]

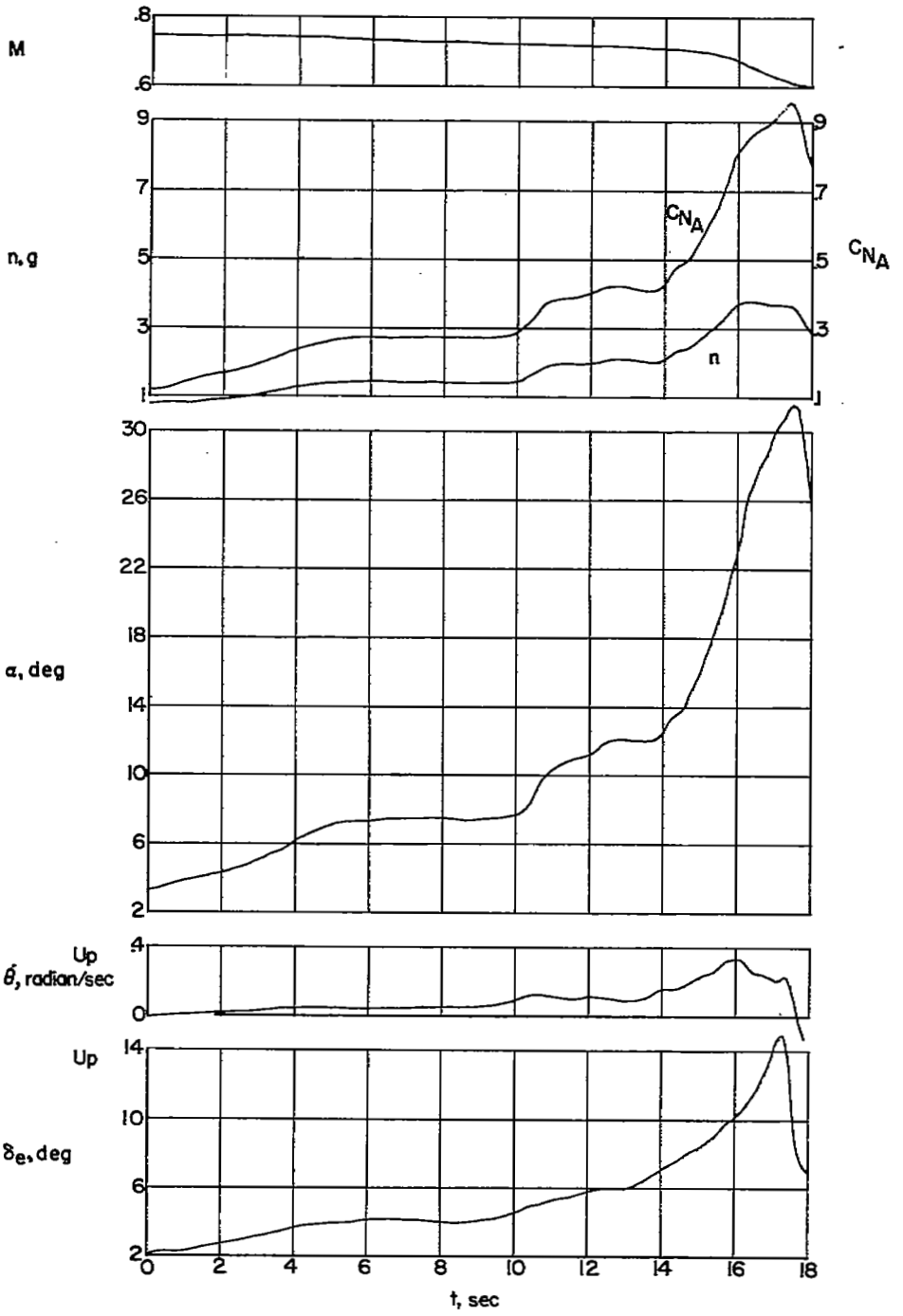

(b) $M \approx 0.70$; $h_p = 36{,}600$ feet; modified fence configuration.

Figure 14.- Continued.

[redacted]

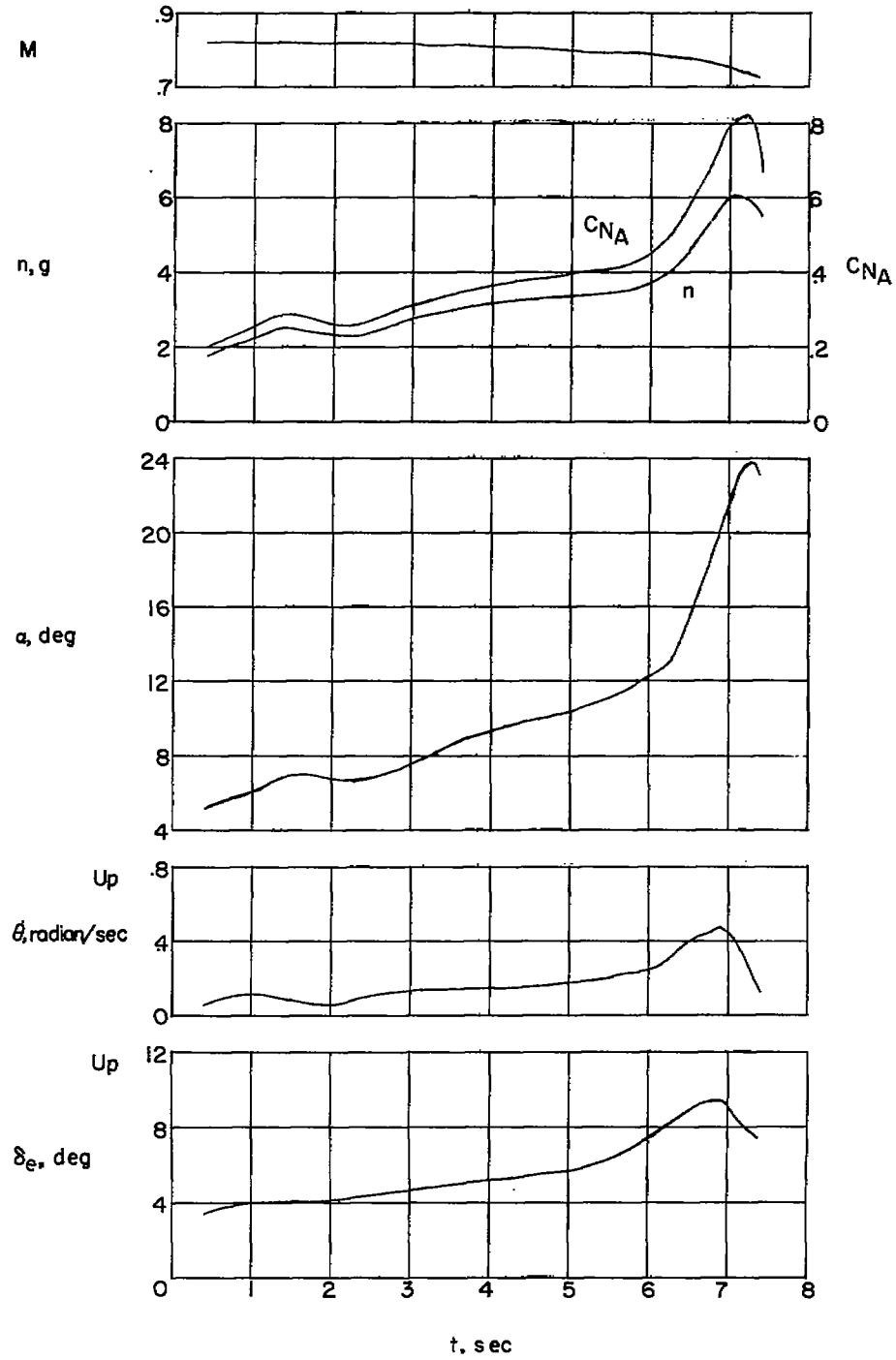

(c) $M \approx 0.80$; h_p = 31,100 feet; modified fence configuration.

Figure 14.- Continued.

[redacted]

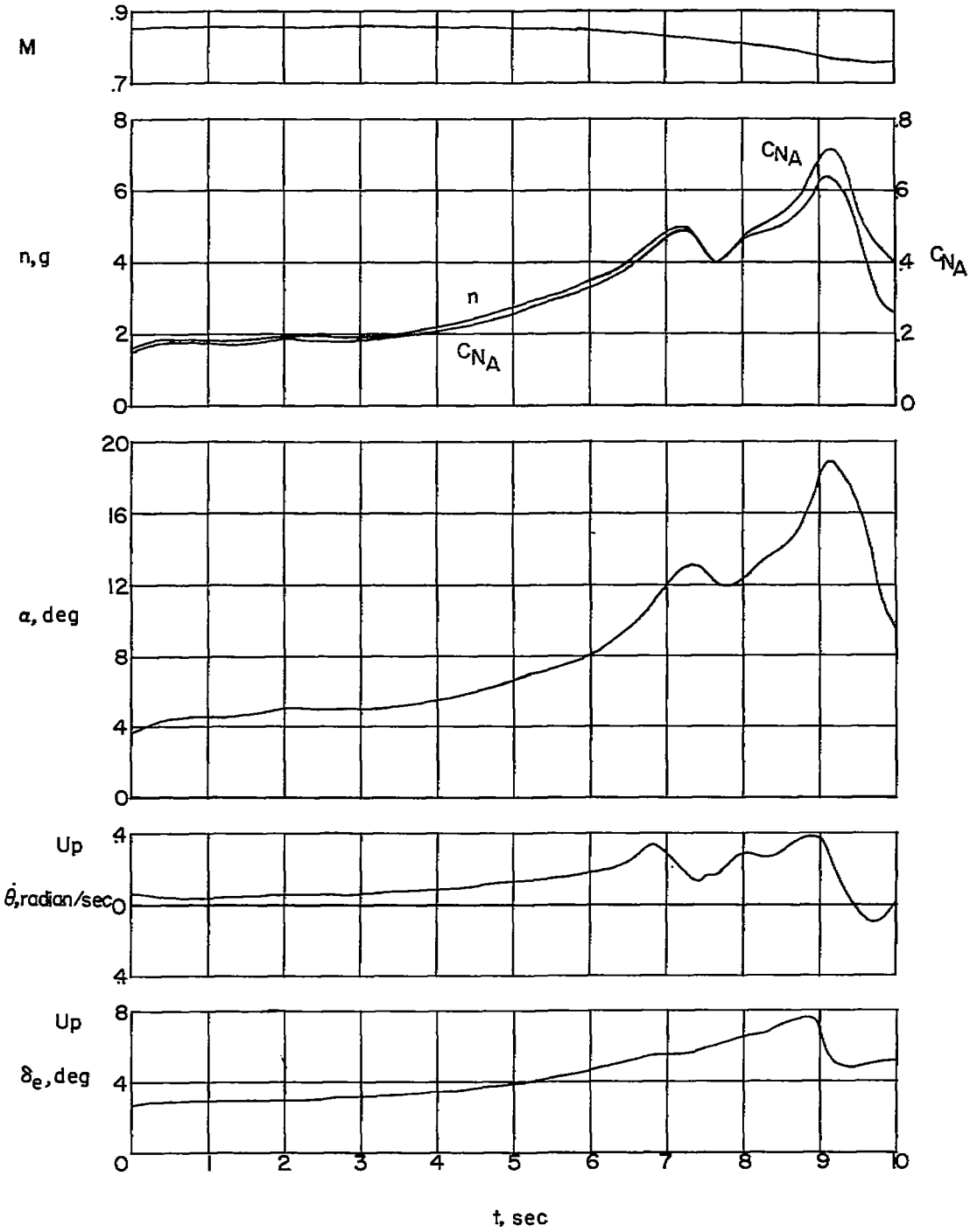

(d) $M \approx 0.85$; h_p = 29,900 feet; basic fence configuration.

Figure 14.- Continued.

[redacted]

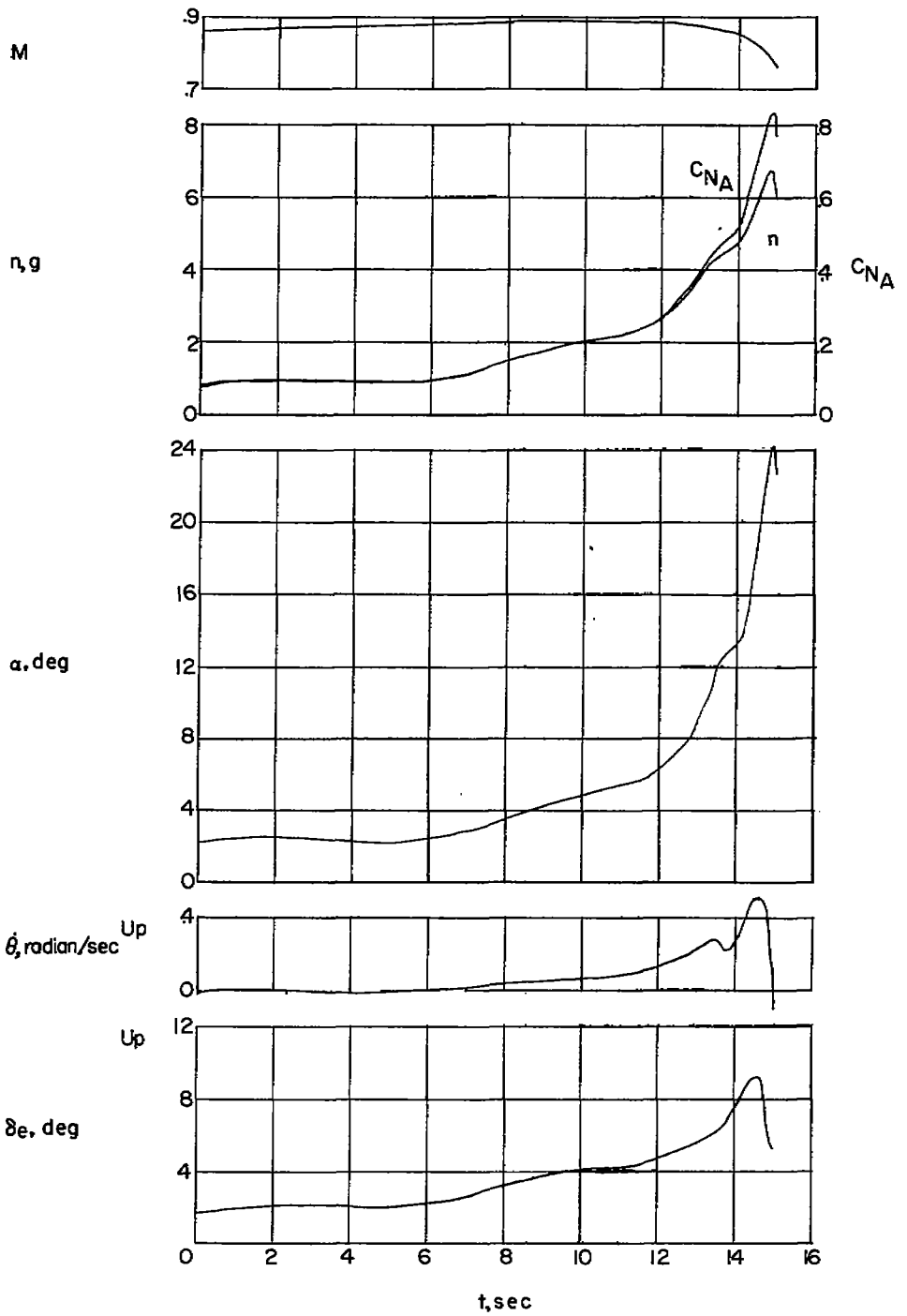

(e) $M \approx 0.85$; h_p = 33,700 feet; modified fence configuration.

Figure 14.- Continued.

[redacted]

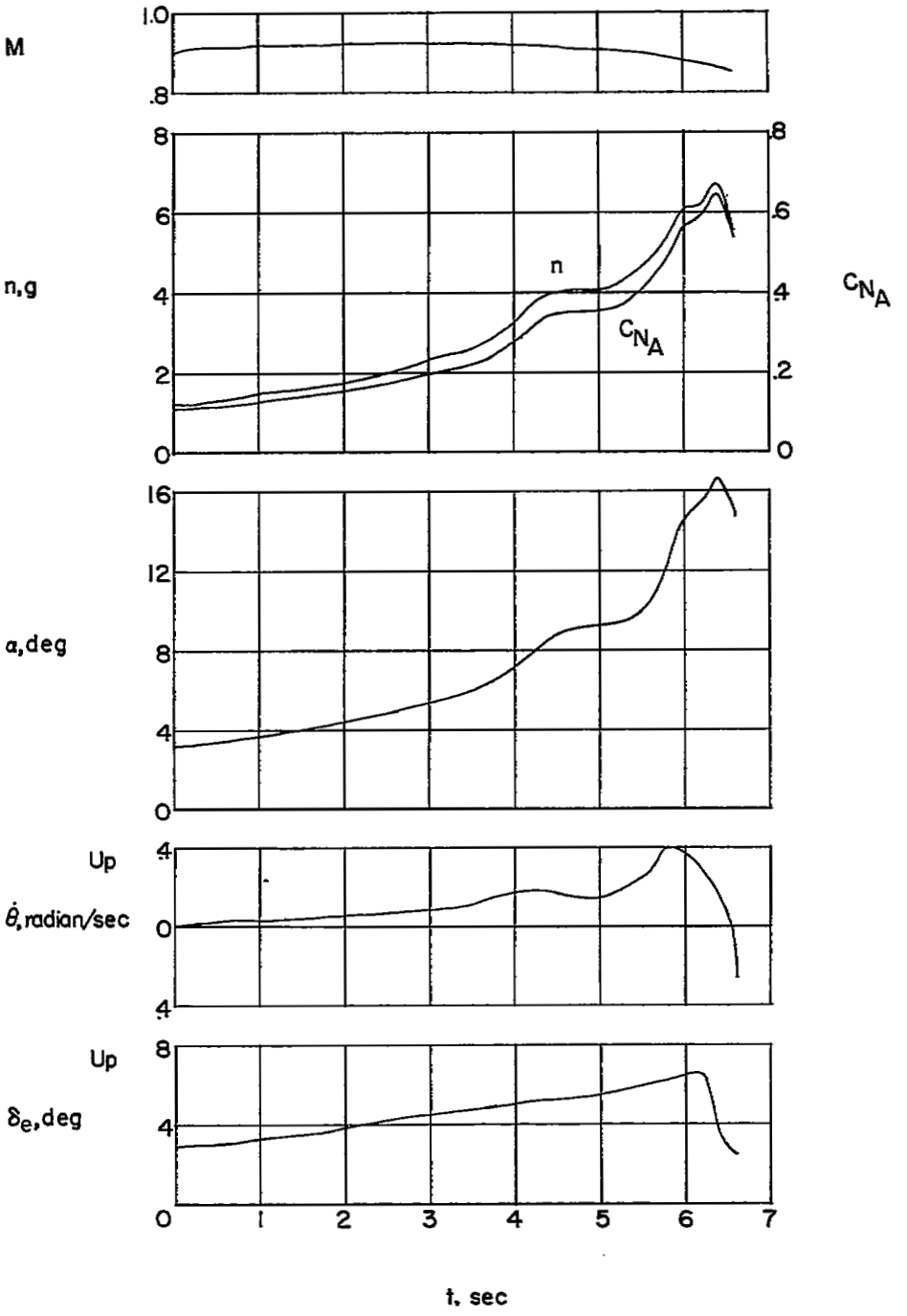

(f) $M \approx 0.90$; h_p = 31,500 feet; basic fence configuration.

Figure 14.- Continued.

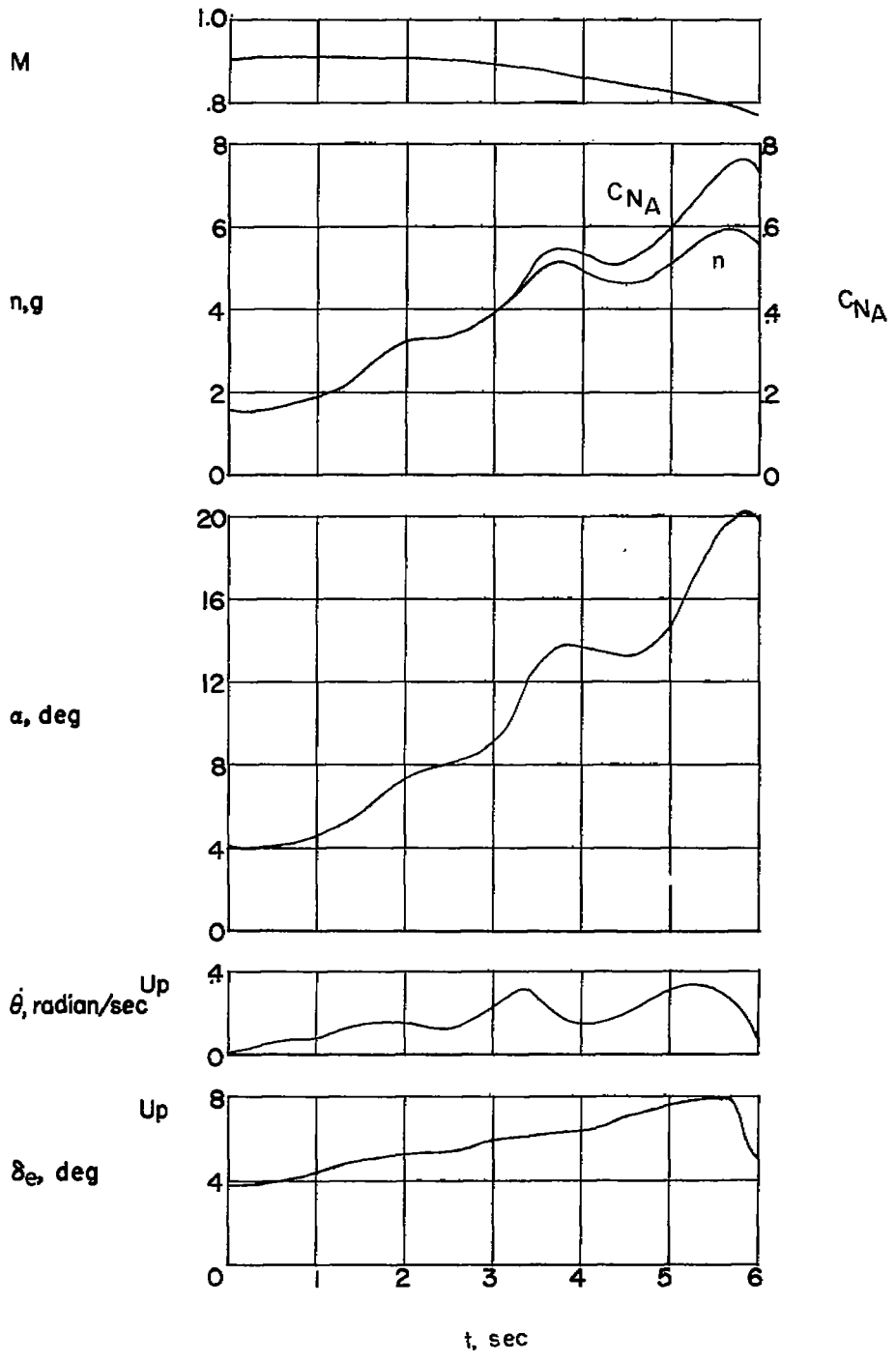

(g) $M \approx 0.90$; h_p = 33,800 feet; modified fence configuration.

Figure 14.- Continued.

[redacted]

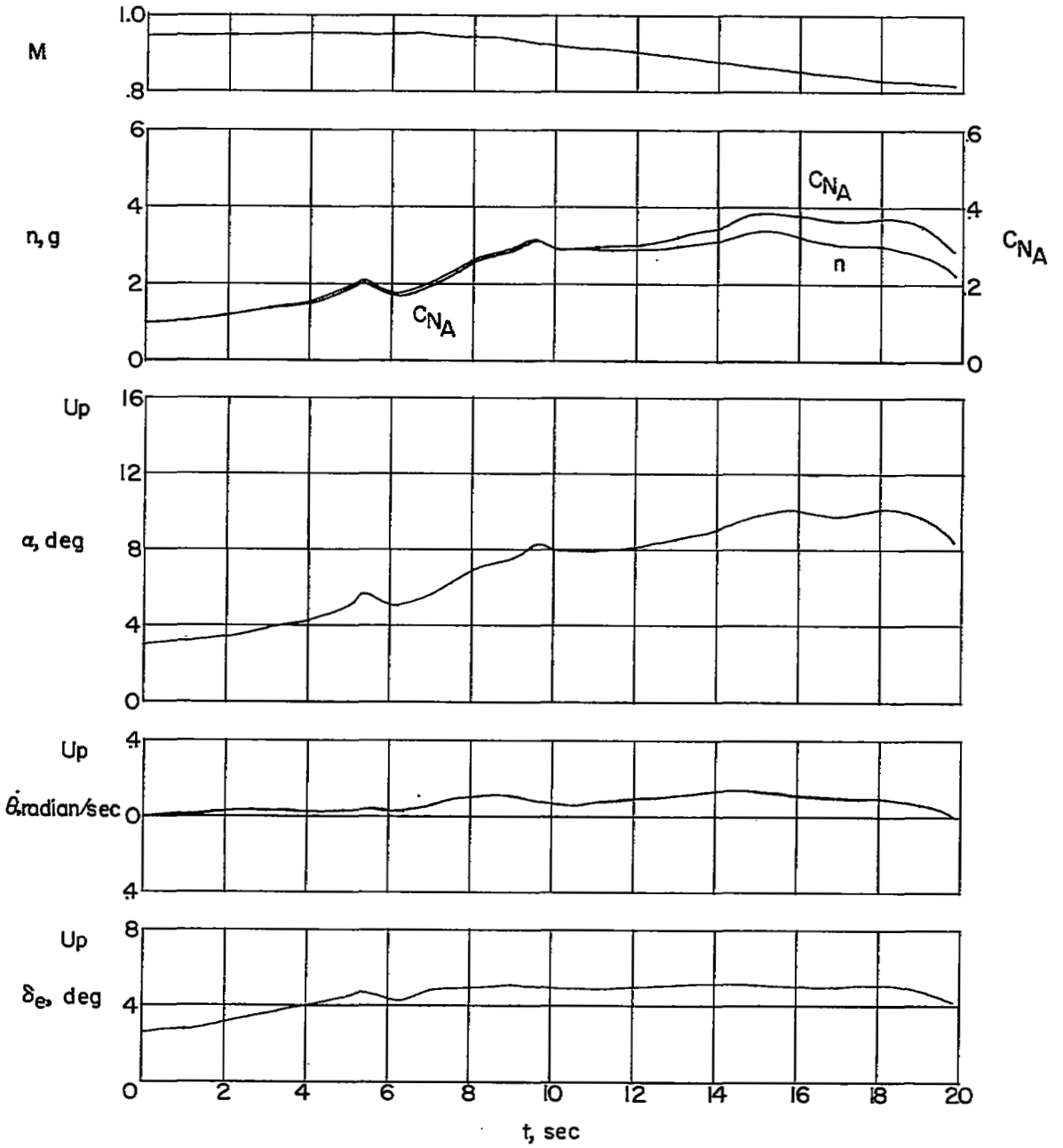

(h) $M \approx 0.95$; h_p = 37,200 feet; basic fence configuration.

Figure 14.- Concluded.

[redacted]

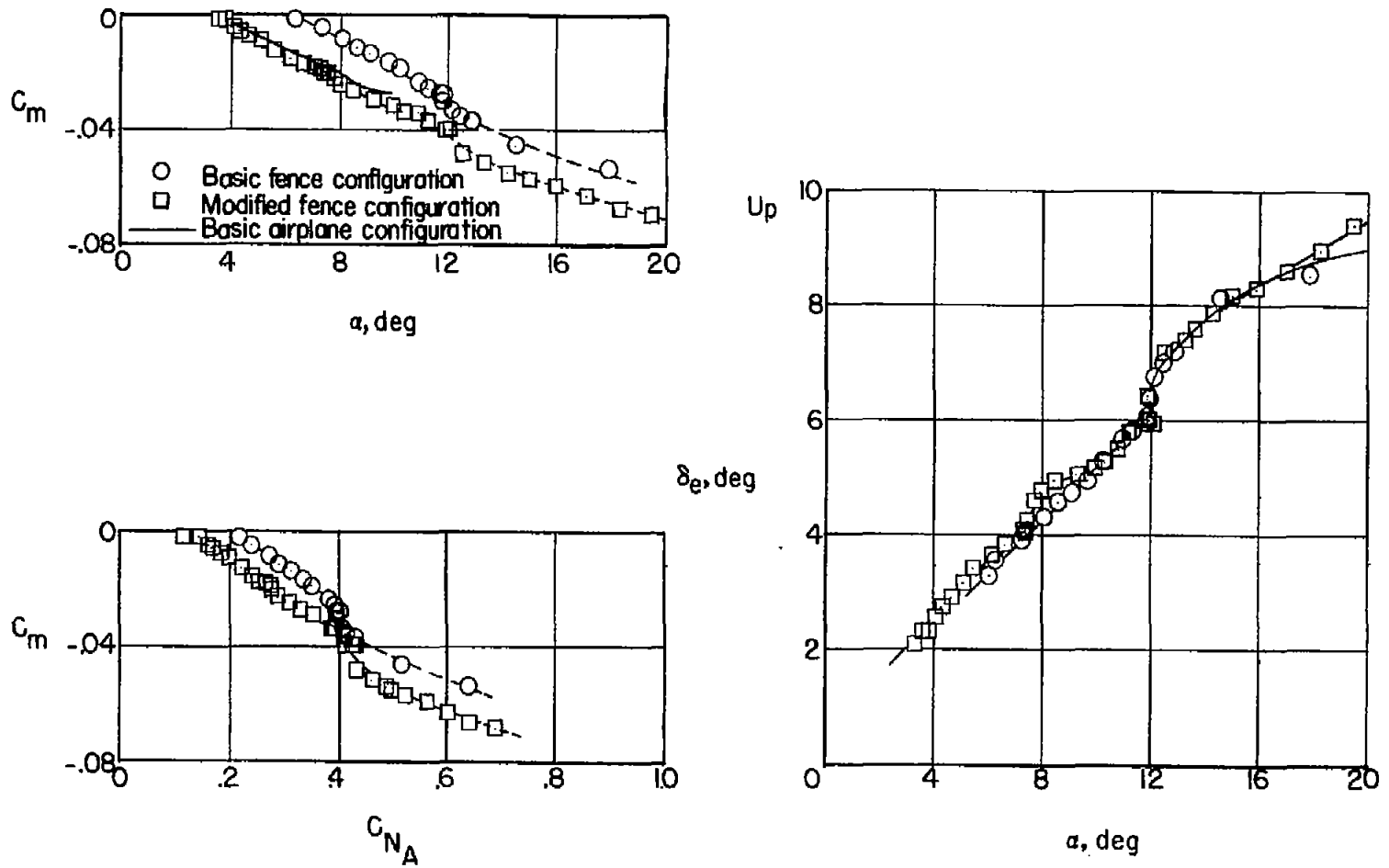

(a) $M \approx 0.70$.

Figure 15.- Maneuvering stability characteristics of the XF-92A airplane at various Mach numbers with wing fences installed.

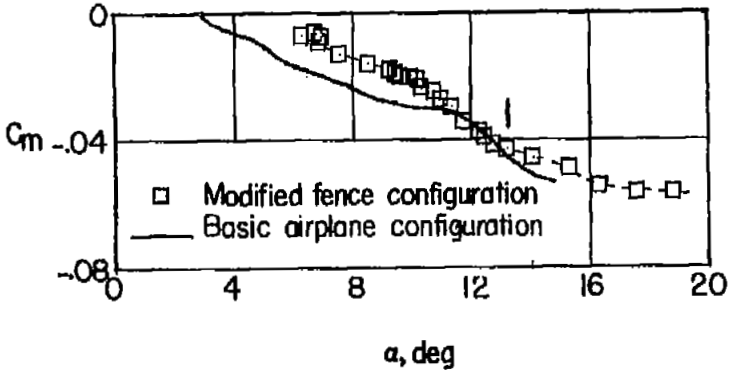

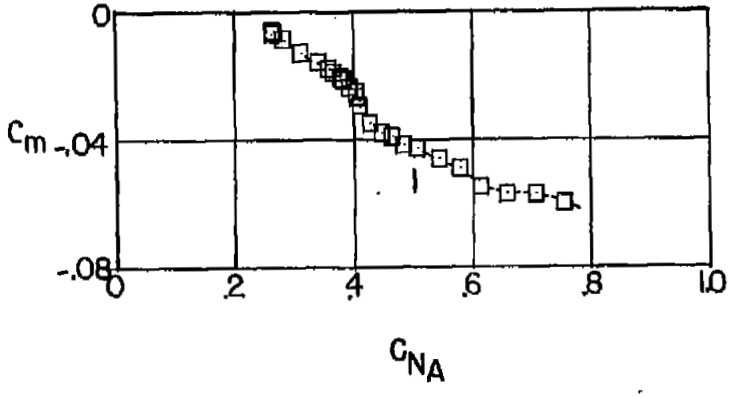

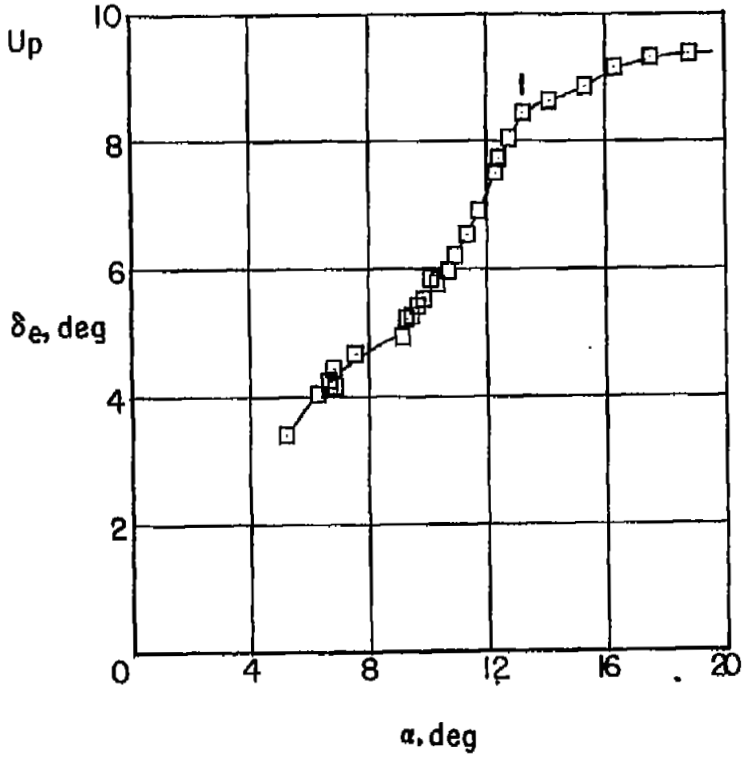

(b) M ≈ 0.80.

Figure 15.- Continued.

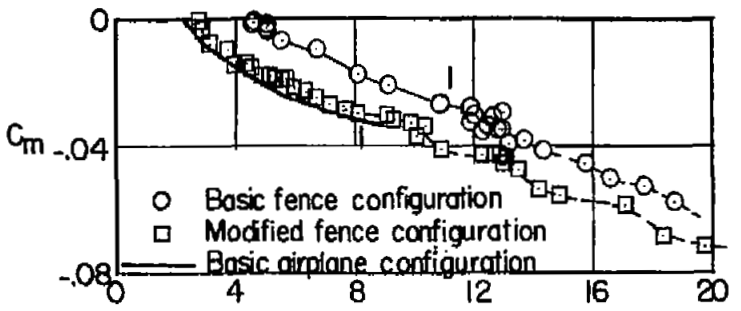

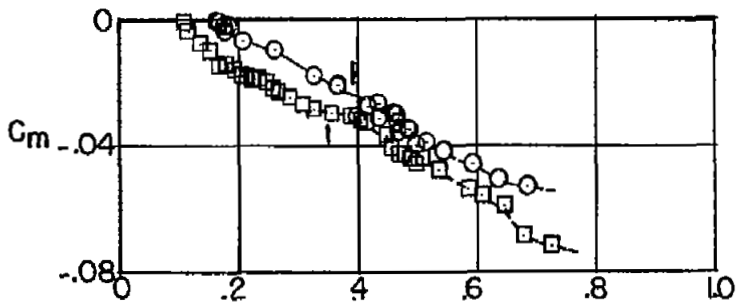

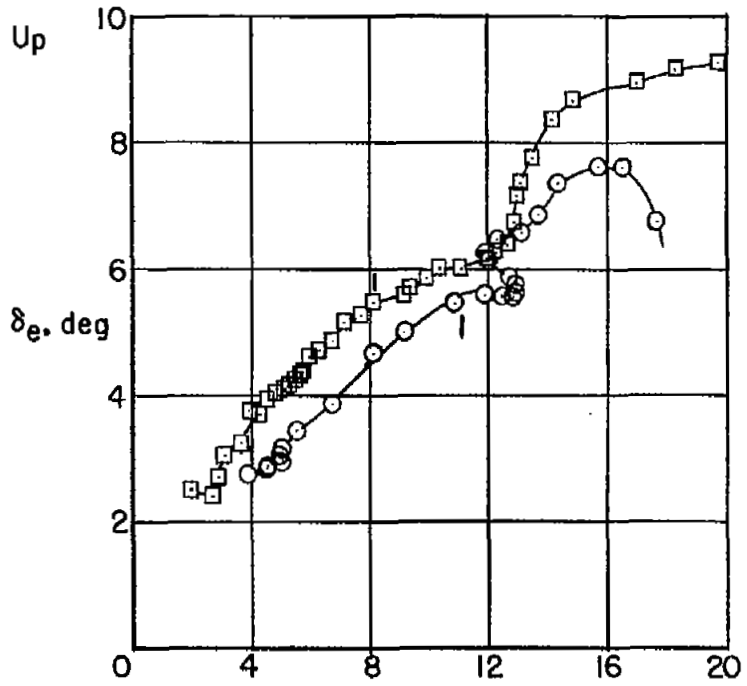

(c) $M \approx 0.85$.

Figure 15.- Continued.

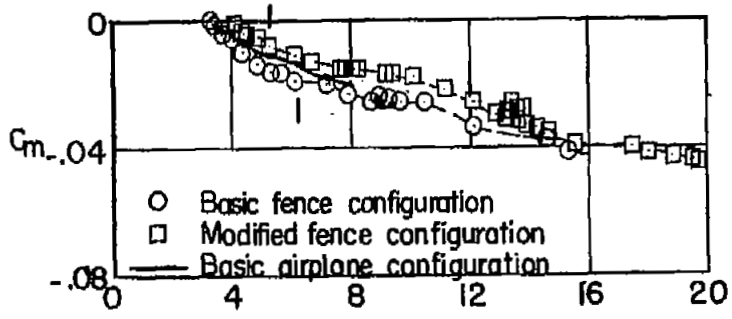

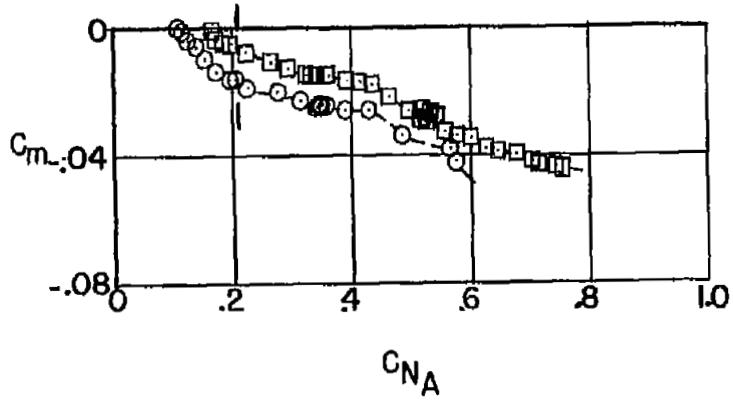

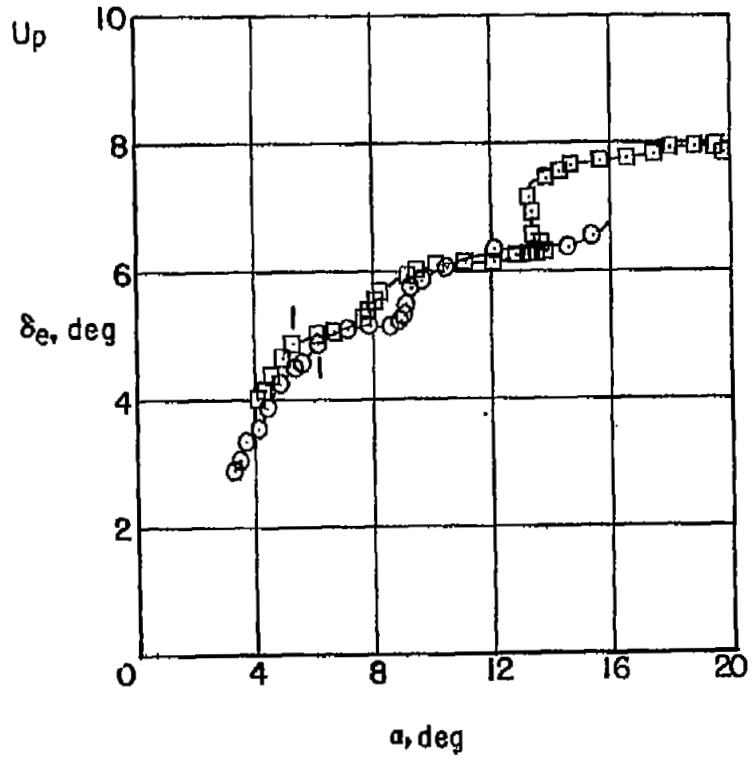

(d) $M \approx 0.90$.

Figure 15.- Continued.

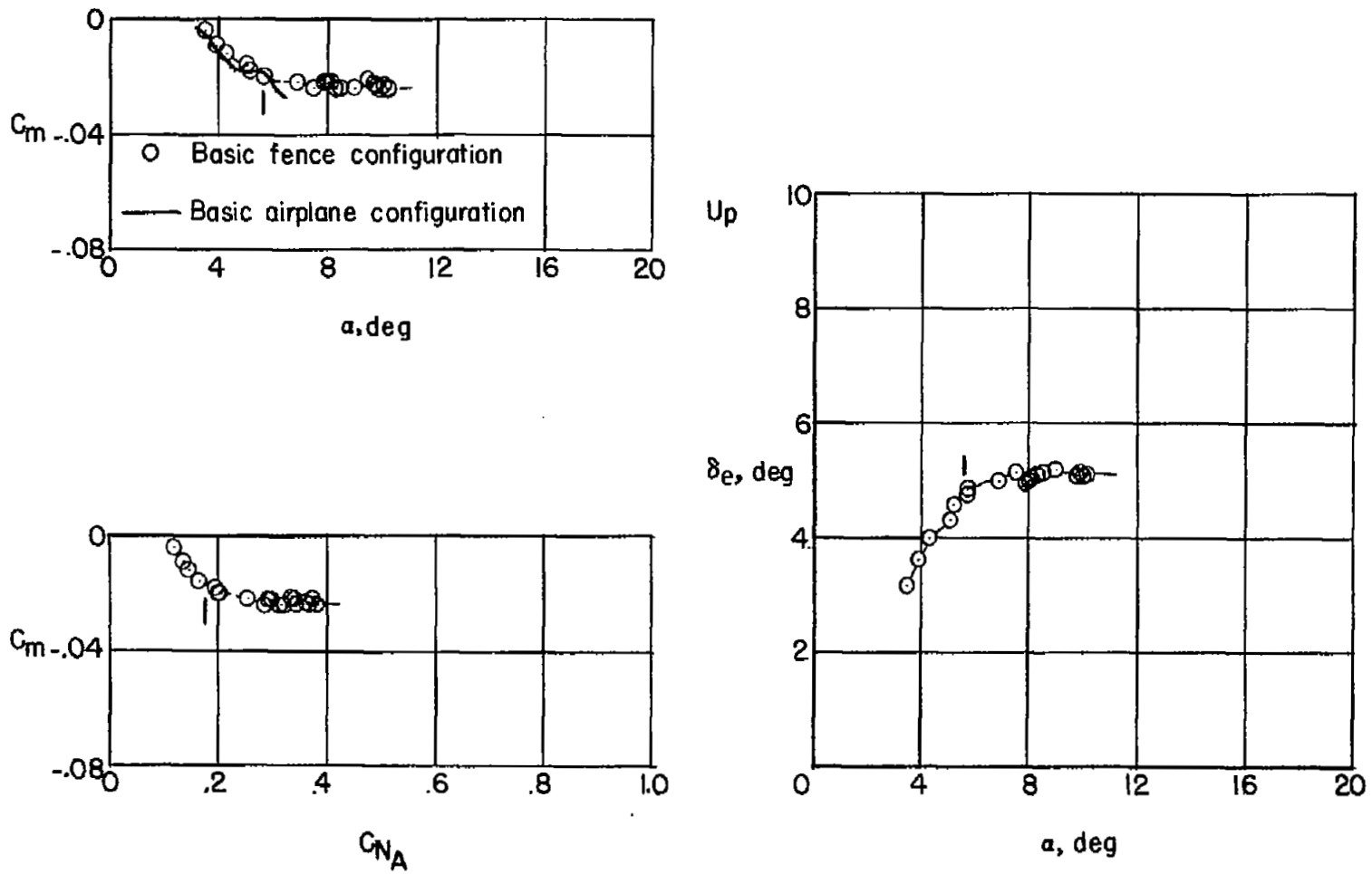

(e) $M \approx 0.95$.

Figure 15.- Concluded.

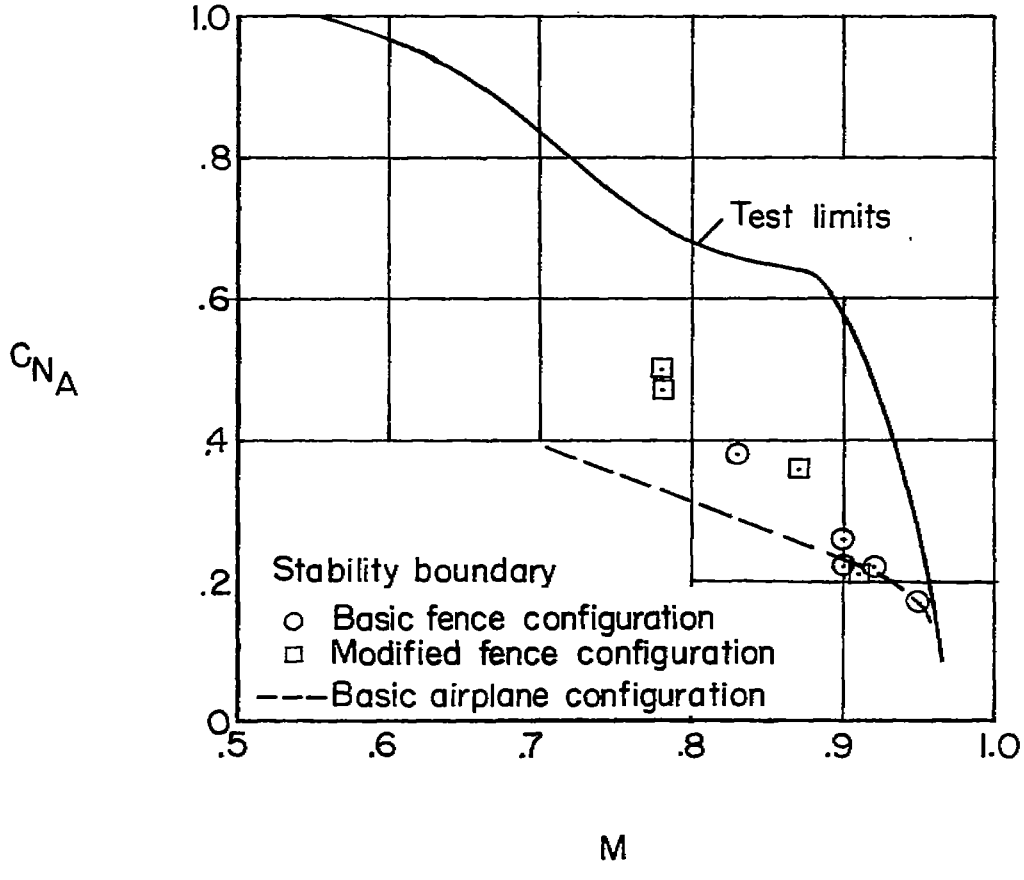

Figure 16.- Boundary for stability decay for the XF-92A with wing fences installed and comparison with the basic airplane configuration.

NACA-Langley - 1-13-55 - 325